

# MOMENTUM MANAGING EPIDEMIC SPREAD AND BESSEL FUNCTIONS

IVAN CHEREDNIK, UNC CHAPEL HILL <sup>†</sup>

**ABSTRACT.** Starting with the power law for the total number of detected infections, we propose differential equations describing the effect of momentum epidemic management. Our 2-phase formula matches very well the curves of the total numbers of the Covid-19 infections in many countries; the first phase is described by Bessel functions. It provides projections for the saturation, assuming that the management is steady. We discuss Austria, Brazil, Germany, Japan, India, Israel, Italy, the Netherlands, Sweden, Switzerland, UK, and the USA, including some analysis of the second waves.

**Key words:** *epidemic spread, epidemic psychology, Bessel functions*

*MSC 2010:* 92B05, 33C10

**1. Our approach and findings.** A system of differential equations is proposed describing the effects of *momentum management of epidemics*, which is in this paper a set of reactive measures mostly based on the latest total numbers of detected infections. The *hard measures* are the key; the most important are the detection and isolation of infected people and closing the places where the spread is the most likely. If their intensity and consistency are high enough, our model provides projections for the saturation of the epidemic spread, followed by the *second phase*, which is essentially a period of modest constant numbers of new infections. The *two-phase formula*, the main output of this paper, was tested well for the spread of *Covid-19* in many countries. The 1st phase is described by Bessel-type functions with surprisingly high accuracy. The exactness of the corresponding formulas for the 2nd phase is even more surprising taking into consideration many factors influencing the management of *Covid-19* in the later stages. The figures from Sections 11, 12 demonstrate our "2-phase solution" for Japan, Israel, Italy, Germany, the Netherlands and UK. The latter and Sweden were the latest in Europe to reach the 2nd phase. The USA

---

<sup>†</sup> October 12, 2020. Partially supported by NSF grant DMS-1901796 and the Simons Foundation.

was close to it, but it was still in phase 1, when it entered the second wave of *Covid-19*. The *second waves* match out theory equally well.

The second phase is when "hard measures" are relaxed or even abandoned. Self-isolation, wearing the protective masks and social distancing become the key. Such and similar *soft measures* reduce the transmission rate, but the 1st phase is the key for reaching the saturation.

Our formula for the total number of cases for the 2nd phase is  $C t^{c/2} \cos(d \log(t))$ :  $t$  is the time,  $d$  reflects the intensity of "soft" measures, and  $c$  is the *initial transmission rate*, which is as follows. The initial growth of the total number of cases is  $\sim t^c$ , where  $c$  is mostly from 2.2 to 2.8 for *Covid-19*, but reached 4.5 – 5.5 for Brazil and India. The number of new daily infections becomes modest during phase 2. Also, asymptomatic (mild) cases begin to dominate, which contributes to diminishing the spread too.

**Focus on risk-management.** We attribute the similarity of the curves of the *total numbers of detected cases* in many countries to the uniformity of the measures employed and to the ways people react to the threat, more specifically, react to the growing numbers of infections.

The total number of cases is generally more reliable and stable than other characteristics of *Covid-19*, though it depends. It is not really important in our approach that they mostly reflect *symptomatic cases* and are frequently underreported. *As far as they influence the decisions of the authorities in charge and our own behavior, they can be used.* Our focus on the epidemic management resulted in algebraic-type formulas for the curves of total cases, which explain very well the surprising uniformity of such curves in so many different places.

We identify 3 basic types of governmental management. The countries in the first group are determined to reach "double-triple digit numbers" of new daily infections, which is our (A)-mode. The second group is when the reduction of hard measures begins upon the first signs of the stabilization of the daily numbers, even if they are high; this is a premature switch to the (AB)-mode or (B)-mode for us. The third group of countries is where "hard" measures are not employed systematically, which can be due to a variety of reasons, including insufficient medical capacities or political decisions.

Some measures are of course always in place: medical help, self-isolation of those who think that they can be infected, various self-imposed limits, and so on. We focus on *active momentum management*.

**Testing our theory.** Our research was organized as follows. The theory and its applications to mode (A), the most aggressive one, were essentially completed around April 15 of 2020. Not too many countries reached the "saturation" by then, but the middle stages matched this

new theory almost with an accuracy of physics laws. The challenge was to understand the later stages.

The parameter  $c$ , the initial transmission rate, can be obtained during the early stages; finding  $a$ , the intensity of hard measures, generally requires the period till the "turning point". Assuming that the measures are steady, this can be sufficient for forecasting the spread, but not always. For instance,  $a, c$  coincided for the UK and the Netherlands. The latter reached the end of phase one after about 45 days (counting from March 13), matching well our Bessel-type formula. This appeared significantly slower in UK, which we attribute to the relaxation of the "hard" measures there after the "turning point". It is even more visible in the USA, where the middle stage *perfectly* matched our formula with the smallest  $c$  we ever observed: 2.2. Then the measures were reduced, phase 2 was not reached, and eventually the USA entered wave 2.

At the end of April, we saw some signs of the switch from mode ( $A$ ) to mode ( $AB$ ) in the USA and UK. This is a transitional mode, where the main measures are "hard", but the response to the current number of infections is as in mode ( $B$ ), not really "aggressive". The corresponding ( $AB$ )-curves, called  $w$ -curves in the paper, were calculated for the USA, UK on May 5. The expected dates of "phase-1 saturations" under the ( $AB$ )-mode were correspondingly May 30 and June 10 for these countries. This worked well for UK, but did not materialize for the USA due to further significant reduction of the hard measures approximately in the middle of May. The economic and societal impact of "hard measures" is of course huge. However long periods of high daily numbers of new infections obviously present significant risks.

Concerning the USA, a period of essentially constant, but high, numbers of new daily cases lasted for some time, mathematically, similar to that in Sweden. However, when processing *automatically* all 50 states individually, we found at the end of May, that about 22 states were already in phase 2, which appeared sufficient to expect the general saturation at 09/19. This projection remained quite stable till the end of June, when the changes with the policies in *almost all* 50 states toward "opening" resulted in a very different scenario.

The number of the states in phase 2 quickly dropped from 22 only to 8: Colorado, Connecticut, Maine, Massachusetts, New Hampshire, New Jersey, New York, Rhode Island as of July 8. Then USA entered the *second wave* at about June 15, with the starting number of total detected cases about  $2M$ .

**The second wave.** Upon subtracting initial numbers, the match with the corresponding Bessel-type solution appeared very good for the 2nd wave, with the transmission rates  $c$  comparable with those for the 1st wave. This was expected in our theory. Our  $c$  is some combination

of the transmission strength of the virus and the "regular" number of contacts in the considered area. A preliminary analysis of about 10 countries, shows that it can somewhat increase. The parameter  $a$ , the intensity of the "hard" measures, certainly diminished significantly;  $1/\sqrt{a}$  is essentially proportional to the time till the saturation. This is not unexpected: the second wave of extensive lockdowns seems not too likely.

According to our automated program, the spread of *Covid-19* remained mild in Western Europe till the middle of July, though the following countries had clear second waves as of July 8: Albania, Bosnia and Herzegovina, Bulgaria, Croatia, Czech Republic, Greece, Kosovo, Luxembourg, Macedonia, Montenegro, Romania, Serbia, Slovakia, Slovenia. Also, Sweden, Poland, Portugal and some other countries did not reach phase 2 at that date. Then the number of new cases increased at the end of July.

We analyze in the paper the current second waves in Israel and the USA. Among other factors, many schools were open in Israel in June and quite a few summer activities for children were held in July-August, which presumably contributed to the high magnitude of the second wave there. This is more complex in the USA, especially because of the "unfinished" 1st wave.

Nevertheless, it appeared that the curves of the total number of cases are very similar to each other in these countries, upon some natural rescaling. This uniformity and good match with our Bessel-type solutions provide of course a confirmation of our approach. It is worth mentioning here that it is not impossible that the measures can be not that "hard" for the second wave to have the same effect, though the *detection-isolation-tracing* remains of course the key.

Our general theory remains essentially unchanged from its first posted variant (April 13). However only now all its main features are confirmed to occur in reality, including the second Bessel-type solutions, and the significance of modes  $(B) - (AB)$ . Let us comment on it.

The second, non-dominating, Bessel-type solutions explained some "bulges" of the curves of total cases, during the early and middle stages in many countries. Generally, *all* solutions of ODE, PDE must occur when used for modeling. Mode  $(B)$  and the  $\log(t)$ -saturation appeared the key in the second phase. The  $(AB)$ -mode is not used much in this paper, but creating "forecast cones" is of obvious importance. Last but not least, the fact that the Bessel-type formulas describe well the *second waves* is a confirmation of our methods.

**Classical theory.** The solutions of the basic classical equation for the number of infections of communicable diseases is with the exponential growth of its solutions, which describes only initial stages of epidemics. The growth is no greater than some power functions in time during the middle stages, so these equations must be changed.

The equally classical *logistic* equations for the spread, as well as the SIR and SID models, assume that the number of infections is comparable with the whole population, which was not really the case with "major epidemics" we faced during the last 100 years. This is mostly due to better disease control worldwide. The *herd immunity* is of course of fundamental importance, but many epidemics were significantly reduced or terminated (well) before it had full effect.

Thus, we must firstly address the *power-type growth of epidemics* except for short initial short periods of exponential growth (if any). This can be clearly seen with *Covid-19*, including sufficiently long periods of essentially linear growth of the total number of infections. And the saturation happens well before the number of infected people becomes comparable with the whole population.

We mostly associate this "polynomiality" with some assumptions on the distribution of infected people, a kind of local herd immunity: infected people do not transmit the virus if *surrounded* by those infected or recovered. However some sociological and biological factors contribute too; see e.g. [CLL, Ch1, Ch2].

Whatever the theoretical foundations, the *power law of epidemics* must be the starting point of any analysis if we want our mathematical models to be up to date, the challenges with *Covid-19* included. Our approach is entirely based on the differential equations that provide the power growth. The key was to extend them to the ones that could be used to model the saturation, which we see with *Covid-19* and other epidemics. Our formulas are not only accurate. They are simple and depend on very few parameters: essentially, the initial transmission rate  $c$ , and the intensities  $a, d$  of the measures for phases 1,2.

**Behavioral aspects.** There is a strong connection of our approach with behavioral science, including *behavioral finance*. Our differential equations are actually from [Ch1] devoted to *momentum risk-taking*, with momentum investing as the main application. The aggressive management of type (A) from Section 2 is an almost direct counterpart of *profit taking* from Section 2.6 of this paper. The measures of type (B) are parallel to the investing regimes discussed in Section 2.4. The key link to financial mathematics is that the *price function* from [Ch1] is a counterpart of the *protection function* in the present paper.

Paper [Ch1] can be considered as some step toward *general purpose artificial intelligence*, the most difficult and ambitious among various AI-related research directions. *Momentum risk-taking* is a very universal concept. We even argue in [Ch1] that the mathematical mechanisms we propose can be present in *neural processes* in our brain; see Section 1.4 there. The ways we manage risks real-time are of course related to behavioral aspects of epidemics.

**2. Two kinds of management.** There is a long history and many aspects of mathematical modeling the epidemic spread; see e.g. [He] for a review. The present paper seems the first one where the momentum management of epidemics is considered the *cornerstone*. To be more exact, our  $c$ , the *initial transmission coefficient*, reflects the transmission strength of the virus and the "normal" number of contacts in the infected areas, so it is "given". However, the second parameter, the intensity  $a$  of the measures, is entirely about the management. The basic management modes are as follows:

- (A) aggressive enforcement of the hard measures, where their intensity is directly linked to the current *absolute* number of infections;
- (B) an approach when the *average* number of infections to date is the trigger and the employed measures are of more palliative nature.

**Hard and soft measures.** To clarify, the main actions of type (A) are testing, detection, and prompt isolation of infected people and those of high risk to be infected, as well as closing places where the spread is the most likely. Wearing protective masks, social distancing, recommended self-isolation, restrictions on the size of events, travel restrictions are typical for (B). The following is important to us.

Mathematically, the modes (A) are (B) are based on different ways to respond to the total number of detected infections: the *absolute* current number of infections is the trigger for (A), whereas the *average* number of infections to date is the key under (B).

The (A)-type approach provides the fastest possible "hard" response to the changes with the number of infections. With (B), we postpone with our actions until the averages reach proper levels, and the measures we implement are "softer". Mathematically, the averages are better protected against stochastic fluctuations, but (B) alone significantly delays the termination of the epidemic, as we will show within our model. There is an analogy with *investing*, especially with *profit taking*: an investor either directly uses the *price targets* or prefers to rely on the so-called *technical analysis*, based on charting averages.

Let us emphasize that by "response" and "actions", we mean not only those by the authorities in charge of the epidemic. Our own ways of reacting to epidemic figures are equally important. We can "monitor" the *total* number of infections and act accordingly, or mostly "consider" this number divided by the time from day 1, some substitute for the number of new daily infections. For instance, when the number of new infections is constant (even high), this can be acceptable for some. On the other hand, this means some steady growth of the total number of infections, which can be troubling if these numbers are already high. Epidemiology has strong roots in behavioral science, psychology, sociology, mass and collective behavior; see e.g. [St].

**Saturation.** Both modes, (A) and (B), are momentum, responding to the latest data. As we will see, both provide essentially the same kind of growth of the total number of infections in the beginning:  $\sim t^c$  in terms of time  $t$  and for the initial transmission rate  $c$ . The main difference is that the solutions of the differential equations of type (A) are *quasi-periodic*: asymptotically periodic functions in  $t$  multiplied by power functions. This automatically grants sufficiently fast "saturation", which is reaching the first maximum. Then they cannot be used for modeling the *total* number of infections: it always increases. For (B), we have  $\log(t)$ -quasi-periodicity, but it reveals itself only in the late stages; it can be really seen with *Covid-19* during *phase two*.

The periodicity of our solutions is not related to the periodicity of the epidemic models based on seasonal factors, various delays and other mechanisms of this nature; see e.g. [HL]. The periodicity and saturation we consider are entirely due to active *momentum* management.

The "forced" saturation of this kind can be unstable. Reducing the measures too much on the first signs of improvement is likely to result in further *waves* of the epidemic, which can be very intensive. This was expected theoretically and now it becomes a serious concern.

**3. Power law of epidemics.** Here and below we will assume that the number of people perceptive to the virus is unlimited, i.e. we do not take into consideration in this paper any kind of saturation when the number of infected people is comparable with the whole population. Accordingly, *herd immunity* and similar factors are not considered. Also, we disregard the average duration of the disease and the durations of the quarantine periods.

The *total number of detected infections* is what we are going to model. This is commonly used; the corresponding data are widely available and seem the most reliable.

For any choice of units, days are the most common, let  $U_n$  be the number of infected individuals at the moments  $n = 0, 1, 2, \dots$ . The simplest equation of the epidemic spread and its solution are:

$$(1) \quad U_n - U_{n-1} = \sigma U_{n-1} \quad \text{for } n = 1, 2, \dots, \quad \text{and } U_n = C(1 + \sigma)^n$$

for some constant  $C$  and the *intensity*  $\sigma$ . Here  $\sigma$  is the number of infections transmitted by an average infected individual during 1 time-unit, assuming that the "pool" of non-infected perceptive people is unlimited. The problem here is that the exponential growth of  $U_n$  can be practically present only during the early stages of epidemics, especially with the epidemics we faced during the last 100 years.

An important factor ignored in (1) is that  $U_n - U_{n-1}$  is actually proportional to  $U_{n-1} - U_{n-p}$ , where  $p$  is the period when the infected people transmit the virus in the most intensive way. Switching to  $p$  as

the time-unit, we arrive at  $U_n - U_{n-1} = \rho(U_{n-1} - U_{n-2})$ , where  $\rho$  is essentially the *basic reproduction rate*  $R_0$ . One has:  $U_n = C_1\rho^n + C_0$  for some constants  $C_{0,1}$ ; so the growth is still exponential for  $\rho > 1$ .

We are going to replace  $U_{n-1} - U_{n-2}$  by  $U_{n-1}/(n-1)$  with some coefficient of proportionality. This can be obviously done if  $U_n$  grows essentially linearly. Generally, the reasons for such a significant change must be and really are of fundamental nature.

**Some psychological aspects.** Presumably, the linear growth of  $U_n$  is not really sufficient to force us, people, to change our behavior, even with epidemics. However, we certainly begin reducing our contacts and consider other protective measures if the *trend* seems faster than linear. This is not only with epidemics. The question is what we mean by "trend" and how we measure it, at conscious and subconscious levels.

The ratio  $U_{n-1}/(n-1)$  seems almost perfect to represent it. Generally,  $(U_{n-1} - U_{n-2})$  gives this, but it may be not what we really use in this and similar decision-making situations. First, such differences or the corresponding derivatives are poorly protected against the random fluctuations of  $U_n$ . Second, momentum decision-making is very intuitive and sometimes entirely subconscious. "Storing and processing" the prior  $U$ -numbers in our brain is more involved than "keeping"  $U_{n-1}/(n-1)$ . Our brain can perfectly process the input like "yesterday number was  $U_{n-1}$  and this took  $(n-1)$  days", though the mechanisms are complicated. The concept of time is quite sophisticated.

Also, let us mention here that the actions of infected people or those who think they can be infected become less chaotic over time and they generally receive better medical help in the later stages, which reduces the transmission of the virus.

**Some biological aspects.** The *viral fitness* is an obvious component of  $\sigma$ . Its diminishing over time can be expected, but this is involved. This can happen because of the virus replication errors, especially typical for *RNA* viruses, which are of highly variable and adaptable nature. The *RNA* viruses, *Covid-19* included, replicate with fidelity that is close to error catastrophe. See e.g. [CJLP, Co] for some review, perspectives and interesting predictions. Such matters are well beyond this paper, but one biological aspect must be mentioned: *asymptomatic cases*.

The viruses mutate at very high rates. They can "soften" over time to better coexist with the hosts, though fast and efficient spread is of course the "prime objective" of any virus. For instance, quarantine measures may "force" the virus to stay longer in a host; mild strains may have advantages. Such softening certainly results in an increase of asymptomatic cases. Since we model the available (posted) numbers  $U_n$ , which mostly reflect the symptomatic cases, the coefficient  $\sigma$  automatically diminishes when the percentage of the asymptomatic



cases increases. Anyway, softening the virus over time contributes to diminishing  $\sigma$ . We will provide more direct "geometric" reasons for the switch from  $\sigma$  to  $\frac{\sigma}{n-1}$  below: some kind of "local herd immunity".

**Master equation revisited.** We arrive at the following equation for the *middle stages of epidemics*, resulting in the power growth (asymptotically) of its solutions:

$$(2) \quad U_n - U_{n-1} = \frac{\sigma}{n-1} U_{n-1}, \quad n = 2, 3, \dots, \quad U_n \approx Cn^\sigma$$

for some constant  $C$ . When  $\sigma = 1$ ,  $U_n$  becomes exactly  $Cn$ .

Actually, it is not that important in this paper what are the exact reasons for dividing  $\sigma$  by the time here, though we suggest some underlying principles. What is the key for us is that the switch from (1) to (2) is a *mathematical necessity*; the exponential growth is unsustainable.

The power growth can be unsustainable long-term too, but such growth is really present in epidemics, *Covid-19* included, especially during the middle stages. Needless to say that power laws are fundamental everywhere in natural sciences. We outlined some behavioral and biological aspects above, but we think that the most plausible explanation of the applicability of (2) is "geometric".

Equation (2) and its differential counterpart serve several seemingly different "situations". One example is *news propagation* from [Ch1]; this is connected with the spread of epidemics. Let us discuss briefly two other examples where the same equation is applicable; they are from [Ch1] too.

**Tree growth.** Equation (2) reasonably describes the height  $U_n$  of a tree in year  $n$  at least for  $\sigma \approx 1$ . The division of  $U_{n-1}$  by  $(n-1)$  can be interpreted as follow. The radius  $r$  of the root system can be assumed proportional to the tree radius. Therefore the root system, which is basically flat, must provide nutrition for the whole tree which is 3-dimensional. We obtain that the growth of a tree during one year is essentially proportional to  $r^2/r^3 = 1/r$  times its prior height,  $U_{n-1}$ . The final assumption is that  $r$  is proportional to  $n$ , which essentially means that the distances between consecutive *tree rings* are constant.

In the beginning and at the end of the life cycle of a tree, this can be different. The volume of the tree can be rather  $r^2$  than  $r^3$  in the very beginning, so the growth can be faster than polynomial. On the other hand, the nutrition the root system provides becomes proportional to  $r$  rather than to  $r^2$  in the later stages. The corresponding term  $\frac{U_{n-1}}{(n-1)^2}$  readily results in the saturation of the tree size, which is well-known and used practically in *bonsai*.

**Neural activities.** We expected in [Ch1] that (2) can serve some basic processes in our brain. The assumptions here are of geometric nature. Let the number of neurons used for a particular task be  $U_n$  at the moment  $n$ . The neural architecture of our brain is obviously about connections (axons) rather than about physical distances between neurons in the brain. Some *auxiliary*  $N$ -dimensional space is needed to present the corresponding "graph" as an image in  $\mathbb{R}^N$  where the distances provide the numbers of connections. Then its *frontier* (border) is the main source of the expansion of this brain activity.

Assuming that the neurons involved in this task are uniformly distributed in the *image* of radius  $r$ , we obtain that  $U_n - U_{n-1}$  is essentially proportional to  $\frac{U_{n-1}}{r}$ , where  $U_n \sim r^\sigma$  for  $\sigma \leq N$ . Finally, we assume that the radius  $r$  grows linearly in time.

Here  $\sigma \leq N$  can be actually any number due to the shape of the image in  $\mathbb{R}^N$ . We arrive at  $U_n - U_{n-1} = \sigma \frac{U_{n-1}}{n-1}$  for proper  $\sigma$ . This model is of course a gross simplification; in contrast to trees and epidemics, we do not know much about the real processes in our brain.

**Back to epidemics.** Following the last example, we represent the population of some area perceptive to the virus as an image in some auxiliary  $\mathbb{R}^N$ ; the numbers of connections/contacts between people then becomes essentially proportional to the *geometric* distances between the corresponding points. The infected individuals fully "surrounded" by infected people or those already recovered do not transmit the disease. Geometrically, they are represented by the points *inside* the image. Its boundary matters the most: these people are better positioned to transmit the virus. In a sense, the *herd immunity* is reached *inside* this image. As above, we assume that the points representing people are distributed uniformly in the image and its radius is basically proportional to the time. We arrive at (2) with  $\sigma \geq 2$ ; if the contacts are mostly between the neighbors then expect  $\sigma \approx 2$ , though the *intensity* of the contacts and the strength of the virus matter too of course.

The uniformity assumption we made is quite standard in physics, say in theory of gases or statistical physics. As everywhere in natural sciences, the simplicity and universality of the resulting equation are of course important considerations. Note that in contrast to  $\sigma$  from (1), the constant  $\sigma$  in (2) and in its differential version are *dimensionless*, i.e. this equation remains the same if we change the time units. This is significant: this constant serves as an exponent.

Recall that we discuss here the epidemic spread without any active management. We see that the polynomial growth of the spread can be "deduced" essentially from one *postulate* of geometric nature: *the "frontier" contributes the most to the epidemic spread.*

**4. Hard measures.** In the realm of differential equations, our starting equation (2) becomes as follows:

$$(3) \quad \frac{dU(t)}{dt} = c \frac{U(t)}{t}, \text{ where } t \text{ is time and } c \text{ replaces } \sigma.$$

We apply Taylor formula to  $U_n - U_{n-1}$ , so  $c$  is "essentially"  $\sigma$ ; we will use mostly  $c$  from now on.

We will model now the impact of aggressive protective measures. The key is the introduction of some *protection function*  $P(t)$ , the total output of the measures.

It is some counterpart of the *price function* in [Ch1]. Essentially, we have two types of measures: (a) isolating infected people, and (b) general diminishing the number of contacts. The are "hard" and "soft" measures, considered above, corresponding to modes (A) and (B); see below and Section 2. Let us begin with the "hard" ones.

**Protection function.** The main "hard" measures are *testing* and *detection* of infected individuals, followed by their isolation and "tracing". They are hard by any standards, especially if there are many cases and the treatment is unknown, as with *Covid-19*.

Generally speaking,  $P(t)$  provides the total numerical "output" of all employed measures. Its derivative gives their *productivity* by definition. For "detection & isolation", we are going to use the following natural definition of  $P$ :

$$P(t) = \frac{1}{c} (\text{the total number of prevented infections from } 0 \text{ to } t).$$

The primary measure here is *testing*; the number  $T(t)$  of tests till  $t$  is what we can really implement and control. The *detection* of infected people is its main purpose, but the number of tests is obviously not directly related to the number of detections, i.e. to the number of *positive tests*, and to the number of resulting *isolations*.

The efficiency of testing is complicated to be measured directly. However, the number of positive tests can be mostly assumed a stable fraction of the total number of tests, especially during the periods of stable growth of the number of total cases. When  $U(t) = \gamma T(t)$  for some  $\gamma$ , finding  $\gamma$  experimentally is not a problem. Accordingly, the system of differential equations will be only for  $U$  and  $P$ .

We assume now that the effect of isolating infected people is approximately linear. More exactly, an infected person isolated at  $t_\bullet < t$  will *not* transmit the disease to  $(t - t_\bullet)$  people till the moment  $t$  (now). This kind of "linearization" is very common when composing differential equations; it does not mean of course that the solutions of our equations will grow linearly.

Thus, if the isolations occur at the moments  $\{t_i\}$ , then these infected individuals will *not* infect  $P(t) = \frac{1}{c} \sum_i (t - t_i)$  people till  $t$  (now). If the latter group of people were not protected, they would infect  $\delta P(t)$  people from  $t$  to  $t + \delta$ , assuming the transmission with the coefficient  $c$  for them. So  $P(t)$  must be subtracted from  $dU(t)/dt$ .

Finally,  $c dP(t)/dt$  is the number of isolated people by construction. We assume it to be  $\alpha U(t)$ , a constant fraction of all infected people, isolated or not. This is another linearization. The coefficient  $a \stackrel{\text{def}}{=} \alpha/c$  is the *intensity* of the isolation process. We arrive at the system:

$$(4) \quad dU(t)/dt = cU(t)/t - P(t), \quad dP(t)/dt = aU(t).$$

The quarantine period, mostly 14 days for *Covid-19*, the duration of the disease and similar factors are disregarded here. However, they are partially incorporated in (3) through  $c$ . Interestingly, such and similar simplifications appeared quite relevant and provided high accuracy of our modeling. We also completely disregard the stochastic nature of epidemics in this paper. Random processes are supposed to be used in a more systematic theory.

With closing factories, schools and other places of high risk, not all people there would be potentially infected if they continued to operate. The *exact* effect of closing (and then reopening) factories and other places where the fast spread of the disease can be expected is almost impossible to estimate. However statistically, this preventive measure is actually no different from the isolation of infected individuals.

Other  $P$ -functions can be used here, but this particular one has a very important feature: *it does not depend on the moments of time when the infected individuals were detected*. If  $P(t)$  depends on  $\{t_i\}$ , the required mathematical tools can be much more involved. Since  $P(t)$  is actually for us to define, it makes sense to "postulate" its main mathematical properties needed to compose the corresponding differential equations; this will be done in (i), (ii) below.

We emphasize that the measures of type (A) impact  $U(t)$  in complex ways: isolating one individual prevents a *ramified* sequence of transmissions. The "soft" measures of type (B), to be considered next, are simpler: they result in a kind of reduction of the  $c$ -coefficient.

**5. Soft measures.** These measures are different from "hard" ones. Wearing protective masks is a key preventive measure of this kind; social distancing, considered mathematically, is of similar type. Now:

*$P(t)$  = the number of infected people who began wearing the masks before  $t$  multiplied by the efficiency of the mask and the  $c$ -coefficient.*

Using the masks for the *whole* population, infected or not, "simply" changes  $c$ ; no new differential equations are necessary. Let  $V(t)$  be the number of infected people wearing the masks. Then  $V(t) \leq U(t)$  and

$$(5) \quad \frac{dU(t)}{dt} = c \frac{U(t)-V(t)}{t} + c' \frac{V(t)}{t} = c \frac{U(t)}{t} - (c-c') \frac{V(t)}{t}$$

for  $c-c' = c(1-c'/c) = c\kappa$ , where  $\kappa$  is the mask efficiency. For instance,  $\kappa = 1$  if  $c' = 0$ , i.e. if the mask is fully efficient for infected people who wear it. The same consideration works for *social distancing*, with  $\kappa$  being the efficiency of the corresponding distance.

An instructional example is when we assume that the fraction of those wearing the masks among all infected people is fixed. If  $V(t) = \nu U(t)$  for some  $0 \leq \nu \leq 1$ , then we have:

$$dU(t)/dt = c(U(t) - \nu U(t))/t + c'\nu U(t)/t = (c - \nu(c - c')) U(t)/t.$$

I.e. this measure results in fact in a recalculation of the  $c$ -coefficient under the proportionality assumption.

Generally speaking, the output of "soft" measures is heavily based on probabilities. However, we only need the following: the greater *intensity* of any measure the greater the reduction of new infections. So we "allow" only one way to control the efficiency of a measure: by changing its *intensity*. The exact mechanisms of its impact are not really needed to know in this approach. Let us formalize this.

**General approach.** From now on, the *intensity* of a measure or several of them will be the main control parameter. As we already discussed, the greater the intensity, the greater the number of isolated infected individuals in (A) or the number of infected people who use the masks in (B). If this dependence is of linear type, which can be expected, the corresponding coefficient of proportionality is sufficient to know. Respectively, the exact definition of the protection function  $P(t)$  is not really needed to compose the corresponding differential equations. What we really need is as follows:

(i) the usage of  $P$  reduces  $dU(t)/dt$ , possibly with some coefficient of proportionality, by  $P(t)/t$  for mode (B), the average of  $P$  taken from  $t = 0$ , or directly by  $P(t)$  under the most aggressive mode (A);

(ii) the derivative  $dP(t)/dt$ , the productivity, is proportional to  $U(t)/t$  under (B), the average number of infections from  $t = 0$ , or directly to  $U(t)$  in the most aggressive variant, which is (A) considered above.

Item (i) has been already discussed. Let us clarify (ii), which provides the *productivity of the measures*  $dP(t)/dt$  in terms of  $U(t)$ .

The proportionality to  $U(t)$  for (A) and  $U(t)/t$  for (B) are the most natural choices. Indeed, the effect of the current number of infections on our actions can be either direct or via some averages. If the averages are used,  $U(t)/t$  is quite reasonable, as we argued above. Mathematically, a relatively fast reaching the saturation requires mode (A) or the transitional mode (AB), which is defined as follows.

We employ "hard" measures as in (A), however follow less aggressive "management formula" for  $dP(t)/dt$  from (B). I.e. this is really some *transitional* mode. As we will see, the epidemic will end under (AB), but the time to the "saturation" will be longer than under (A). If only (B) is used, this is uncertain.

**6. Type (B) management.** Let  $t = 0$  be the starting point of the management; so we can assume that  $P(0) = 0$ . The following normalization is somewhat convenient:  $u(t) \stackrel{\text{def}}{=} U(t)/U(0)$  and  $p(t) \stackrel{\text{def}}{=} P(t)/U(0)$ , i.e.  $u(0) = 1$  and  $p(0) = 0$ . Recall that  $U(t)$  and  $P(t)$  are the number of infections at the moment  $t$  and the corresponding value of the  $P$ -function. Here  $P$  is naturally for the sum of all measures in the considered mode, the sum of their  $P$ -functions.

Obviously mode (A) is significantly more aggressive than (B). Philosophically, the smaller interference in natural processes, which is under (B), the better: the effect will last longer. But with epidemics, we cannot afford waiting too long.

**Type (B) equations.** As it was stated in Section 4, we couple (i) of type (B), which is relation (5), with (ii) for the same mode. I.e. the derivative of  $u(t)$  will be "adjusted" by  $-p(t)/t$  and, correspondingly, the rate of change of  $p$  will be taken proportional to  $u(t)/t$ . This means that the *impact of  $u(t)$  to  $p(t)$  and vice versa goes through the averages*; i.e. the response to  $u(t)$  is not "immediate" as in (A).

Note that the exact  $-p(t)/t$  (later,  $-p(t)$ ) in the equation for  $du(t)/dt$ , i.e. without a coefficient of proportionality, is a matter of normalization. This coefficient can and will be "moved" to the second equation.

The equations under (B) become as follows:

$$(6) \quad \frac{du(t)}{dt} = c \frac{u(t)}{t} - \frac{p(t)}{t},$$

$$(7) \quad \frac{dp(t)}{dt} = \frac{a}{t} u(t).$$

Here  $c$  is the initial transmission coefficient, and  $a$  is the intensity of the protection measure(s). This system can be readily integrated.

Substituting  $u(t) = t^r$ , the roots of the characteristic equation are  $r_{1,2} = c/2 \pm \sqrt{D}$ , where  $D = c^2/4 - a$ . Accordingly, when  $D \neq 0, t > 0$ :

$$(8) \quad u(t) = C_1 t^{r_1} + C_2 t^{r_2} \quad \text{if } D > 0 \text{ for constants } C_1, C_2, \text{ and}$$

$$(9) \quad u(t) = t^{\frac{c}{2}} (C_1 \sin(\sqrt{-D} \log(t)) + C_2 \cos(\sqrt{-D} \log(t))) \quad \text{if } D < 0,$$

where the constants are adjusted to ensure the initial conditions. Note that a proper branch of log must be chosen for  $t$  near zero.

So for  $a < c^2/4$ , the initial  $t^c$  (for  $a = 0$ ) will be reduced up to  $t^{r_1}$  with  $c/2 < r_1 < c$ . When  $a > c^2/4$ , the power growth is always of type  $t^{c/2}$ , and the period of sin and cos with respect to  $\log(t)$  is  $2\pi/(\sqrt{a - c^2/4})$ . The corresponding "saturation" is defined as the first  $t$  such that  $du(t)/dt = 0$ ; here  $t^{c/2}$  obviously contributes.

**Positivity of  $du/dt$ .** The control parameter  $a$ , the intensity, is actually not arbitrary. To see this let us invoke  $v(t) = V(t)/U(t_0)$ , where  $V(t)$  is the number of infected people wearing the protective masks. It was used in the definition of  $P$ :  $P(t) = \kappa c V(t)$ , where  $\kappa$  is the efficiency of the mask (from 0 to 1). We then have:

$$(10) \quad \frac{du(t)}{dt} = c \frac{u(t)}{t} - \kappa c \frac{v(t)}{t}, \quad \frac{dv(t)}{dt} = \frac{a}{\kappa c} \frac{u(t)}{t}.$$

Here  $v(t) \leq u(t)$  by the definition. This inequality generally provides no restriction on the derivatives. However, if  $v(t)$  is essentially proportional to  $u(t)$ , there are some consequences. Let us assume that  $v(t) \sim \gamma u(t)$ . Then we obtain the relation:  $a = c^2 \kappa \gamma (1 - \kappa \gamma)$ . Accordingly, the maximal value of  $a$  is  $a_{max} = \frac{c^2}{4}$  in this case, which is at  $\kappa = \frac{1}{2\gamma}$  provided that  $1 \geq \gamma \geq \frac{1}{2}$ . This gives  $D = 0$  for  $\gamma = 1$ , i.e. this is the case when all wear the masks of efficiency 1/2; then  $u(t) = C t^{c/2}$ , which is obvious from the definition of  $\kappa$ .

Generally,  $du(t)/dt \geq c(1-\kappa)u(t)/t$ , since  $v(t) < u(t)$ , and  $d\tilde{u}(t)/dt \geq 0$  for  $\tilde{u}(t) = u(t)t^{c(\kappa-1)}$ . Thus the solutions  $u(t)$  from (8)&(9) qualitatively grow faster than  $t^{c(1-\kappa)}$  due to (8).

Using the  $\log(t)$ -periodicity (if present), the *(B)-type saturation points* is the first maximum of  $u(t)$ . We must stop using  $u(t)$  after this, because it will begin to decrease. This *(B)-saturation* appeared an important factor during the *second phase* of our "2-phase solution". If the *first phase*, which is under (A), reaches its saturation and results in a relatively small numbers of new daily infections, then mode (B) will governs "the rest". The countries then almost automatically switch to "soft" measures. See Section 11.

**7. Type (A) management.** The most "aggressive" model of momentum management is of type (A), described by system in (4). We replace the average  $p(t)/t$  in (6) by  $p(t)$ , and  $u(t)/t$  by  $u(t)$  in (7). Actually, the first change affects the solutions greater than the second. One has:

$$(11) \quad \frac{du(t)}{dt} = c \frac{u(t)}{t} - p(t),$$

$$(12) \quad \frac{dp(t)}{dt} = a u(t).$$

Solving system (11)&(12) goes as follows:

$$(13) \quad t^2 \frac{d^2 p}{dt^2} - ct \frac{dp}{dt} + et^2 p = 0 = t^2 \frac{d^2 u}{dt^2} - ct \frac{du}{dt} + et^2 u + cu,$$

$$(14) \quad u = A_1 u^1 + A_2 u^2, \quad u^{1,2}(t) = t^{\frac{1+c}{2}} J_{\alpha_{1,2}}(\sqrt{at}) \quad \text{for } \alpha_{1,2} = \pm \frac{c-1}{2}.$$

Here the parameters  $a, c$  are assumed generic,  $A_{1,2}$  are undermined constants, and we use the *Bessel functions* of the first kind:

$$J_\alpha(x) = \sum_{m=0}^{\infty} \frac{(-1)^m (x/2)^{2m+\alpha}}{m! \Gamma(m+\alpha+1)}.$$

See [Wa] (Ch.3, S 3.1). We will also need the asymptotic formula from S 7.21 there:

$$J_\alpha(x) \sim \sqrt{\frac{2}{\pi x}} \cos\left(x - \frac{\pi\alpha}{2} - \frac{\pi}{4}\right) \quad \text{for } x \gg \alpha^2 - 1/4.$$

It gives that  $u^{1,2}(t)$  are approximately  $\mathcal{C} t^{c/2} \cos(\sqrt{at} - \phi_{1,2})$  for some constant  $\mathcal{C}$  and  $\phi_{1,2} = \pm \frac{c-1}{2}\pi + \frac{\pi}{4}$ .

**Quasi-periodicity.** We conclude that for sufficiently big  $t$ , the function  $u(t)$  is basically:

$$(15) \quad u(t) \approx t^{c/2} (A \sin(\sqrt{at} + \pi c/2) + B \cos(\sqrt{at} - \pi c/2)),$$

for some constants  $A, B$ . So it is *quasi-periodic*, which means that the periodicity is up to a power function and only asymptotically; the asymptotic  $t$ -period is  $\frac{2\pi}{\sqrt{a}}$ .

In our setting,  $u(t)$  must always grow, so  $du(t)/dt \geq 0$ . The technical end of phase one is when  $u(t)$  reaches its first maximum;  $\frac{\pi}{2\sqrt{a}}$  is a reasonable *estimate*, but not too exact. For instance,  $u(t) =$



$t^{c/2+1/2}J_{(c-1)/2}(\sqrt{at})$  for  $c = 2.2, a = 1/5$  reaches its first maximum at about  $t = 4.85$ , not at  $\frac{\pi}{2\sqrt{a}} = 3.51$ ; see Figure 1.

**Transitional mode.** It can be applicable to model the epidemic spread when hard measures are certainly used, but are applied "cautiously". This mode is transitional between (A) and (B): one replaces (12) by  $dp(t)/dt = au(t)/t$ , but couple it with the equation for  $du(t)/dt$  from mode (B), which is (6):

$$(16) \quad \frac{dw(t)}{dt} = c \frac{w(t)}{t} - p(t), \quad \frac{dp(t)}{dt} = b \frac{w(t)}{t},$$

where we replaced  $u(t), a$  by  $w(t), b$ ; the  $c$  remains unchanged. It was called *transitional (AB)-mode* at the end of Section 4. Actually, this mode is the part of the theory practically tested the least.

It is aggressive enough to provide the saturation, and better protected against fluctuations than (A). This makes sense practically; let us see what this gives theoretically.

The system remains still integrable in terms of Bessel functions; see formulas (2.20), (2.21) in [Ch1]. The leading fundamental solution is

$$(17) \quad w^1(t) = t^{(c+1)/2} J_{c-1}(2\sqrt{bt}), \quad \text{where } c > 1.$$

The second one is  $w^2(t) = t^{(c+1)/2} J_{1-c}(2\sqrt{bt})$ . One has:

$$(18) \quad u^1(t) \approx t^c \frac{(\sqrt{a}/2)^{(c-1)/2}}{\Gamma((c-1)/2)}, \quad w^1(t) \approx t^c \frac{(\sqrt{b}/2)^{c-1}}{\Gamma(c-1)},$$

when  $t$  is sufficiently close to zero. Practically, they are "almost" proportional with the coefficient calculated from (18) in sufficiently large intervals of  $t$ , not only for  $t \sim 0$ . This is important for forecasting.

The quasi-periodicity will be now with respect to  $t^{1/2}$  and the corresponding asymptotic period will be  $\pi/\sqrt{a}$ . I.e. the process of reaching the saturation is "slower" than for (A), but still significantly faster than for (B), where the "mathematical periodicity" (if any!) is in terms of  $\log(t)$  in (9). This perfectly matches the qualitative description of (AB) as a transition from (B) to (A).

Actually we have a family  $(AB)_\mu$  for  $-1 \leq \mu < 1$  of such modes, described by the system

$$(19) \quad \frac{dw(t)}{dt} = c \frac{w(t)}{t} - p(t)/t^\mu, \quad \frac{dp(t)}{dt} = b \frac{w(t)}{t}.$$

Here the usage of the term  $p(t)/t^\mu$  means that the impact of one isolation of an infected individuals grows non-linearly over time, which actually makes sense. Assuming that  $c > 2$ , the dominant solution is:

$$(20) \quad w(t) = t^{\frac{c+1-\mu}{2}} J_{\frac{c}{1-\mu}-1} \left( \frac{2\sqrt{b}}{1-\mu} t^{(1-\mu)/2} \right), \quad w \sim t^c \quad \text{for } t \approx 0.$$

The second one is for  $1 - \frac{c}{1-\mu}$ ; we follow [Ch1]. When  $\mu = -1$ , the argument of  $J$  is  $\text{const} \cdot t$ , and we arrive at some counterpart of  $u(t)$ .

**Connection to statistical framework.** The solution  $t^r$  for  $r = c$  of our starting equation (2) is the square root of the *variance*  $\text{Var}(B^H)$  of the *fractional Brownian motion*  $B_H(t)$  (*fBM* for short) for the *Hurst exponent*  $H = r$ . It becomes  $r = r_{1,2}$  for the solutions from (8). Alternatively, the parameter  $r$  can be obtained from the self-similarity property of *fBM*:  $B_r(ts) \sim t^r B_H(s)$ . *Qualitatively* the connection with our approach is that the expected (percent) growth of the epidemic spread is essentially proportional to the standard deviation of the corresponding stochastic process. The important conclusion is that the *volatility of the spread is directly related to  $r$* , which of course can be expected qualitatively.

One can try to introduce generalized *fBM* for the *full* solutions from (9), or for our  $u(t), w(t)$  in terms of Bessel functions. See e.g. [Che] for the theory of mixed fractional Brownian motion and its applications in financial mathematics, which is related to our modeling here.

A more systematic way to link our ODE to SDE, Stochastic Differential Equations, is via the Kolmogorov-type equations for the *transition probability density*; see e.g. equation (1.7) from [Kat] for the definition of *Bessel processes*. This is beyond the present paper. Obviously the detailed analysis of our ODE and their applications for the spread of epidemics, what we are doing in this paper, is necessary before we can go to the level of random processes.

**8. Using the  $u$ -curves.** In the range till April 14 the graphs of our solutions  $u(t)$  matched surprisingly well the *total* number of infections in the examples we provide. The starting moments where when these numbers began to grow "significantly"; these moments are approximately around March 16 for the USA and UK, March 13 for Switzerland, and March 7 for Austria. Only  $u^1$  is used in this section.

Here and below, <https://ourworldindata.org/coronavirus> is the main source of the *Covid-19 data*; this site is updated at about 11:30 London time. We also use "worldometers". From now on,  $x =$

days/10. As for  $y$ , to improve the readability it will be always the number of total (detected) cases divided by a proper power of 10.

**The USA data.** The scaling coefficient 1.7 in Figure 1 is adjusted to match Figure 2 for the United States. For the USA, we set  $y = \text{infections}/100K$ , and take March 17 the beginning of the period of "significant growth". Then  $c = 2.2$ ,  $a = 0.2$  appeared perfect in the considered range.

Recall that  $c$ , the initial transmission rate, reflects the virus transmission strength and the way people respond to the current numbers of infections. These numbers of course depend on the information provided by the authorities in charge and mass media.

The *dots* in all figures show the corresponding actual *total* numbers of infections. They *perfectly* match  $u(t) = 1.7 t^{1.6} J_{0.6}(t\sqrt{0.2})$  in Figure 1. Accordingly, assuming the same intensity of hard measures, the projection for the USA was:  $t_{top} = 4.85$  (48.5 days from 03/17 till the saturation at May 5) with  $u_{top} = 10.3482$ , i.e. with 1034820 infections (it was 609516 at 04/15). This did not happen; see below.

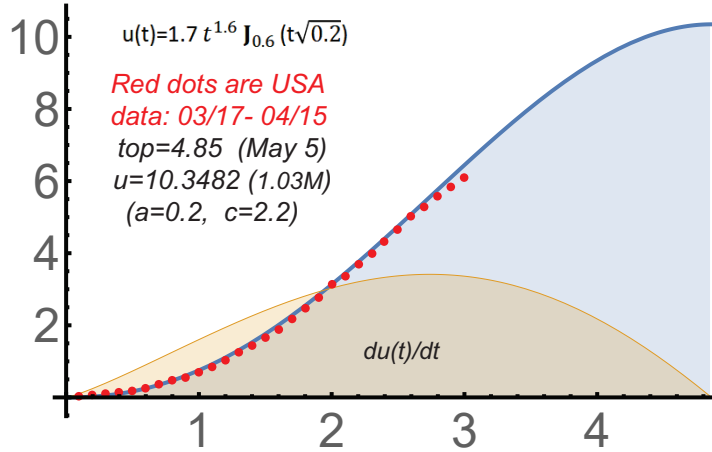


FIGURE 1.  $u(t) = 1.7 t^{(c+1)/2} J_{(c-1)/2}(\sqrt{at})$  for  $c = 2.2, a = 0.2$

The saturation at  $t = t_{top}$  is of course a technical one, not the end of the spread of *Covid-19*, even if it is reached. The data from quite a few other countries demonstrated that some modest linear-like growth of the total number of cases can be expected after  $t_{top}$ , and then the *second phase* begins. The epidemic remains far from over.

With these reservations, our graphs and many others we considered for *Covid-19* demonstrate that Bessel functions describe very well the *first phase*, the period of "aggressive management" of type (A).

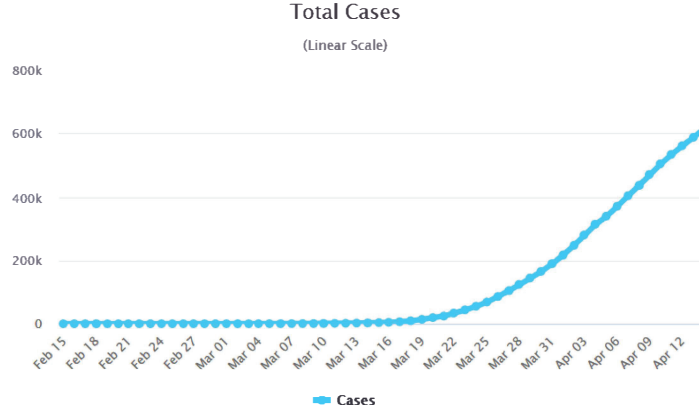


FIGURE 2. Covid-19 in the United States

”Hard” measures are of course not the only force during phase 1. They are *always* combined with ”soft” ones. There are other factors and different stages. The graph for Switzerland is used to demonstrate various stages during this phase in Figure 5 below.

Assuming that Bessel-type functions model well the period of the intensive growth, one can try to ”capture” the parameters  $c, a$  before or near the turning point of the epidemic. If  $a, c$  are known, the first local maximum of the corresponding Bessel function times  $t^{c/2+1/2}$  gives an estimate for the possible ”saturation”, the technical end of phase 1. This is of course under the steady ( $A$ )-type management, which appeared the case in sufficiently many countries.

In the data we provide,  $a$ , the intensity of ( $A$ )-measures, is 0.2 for the USA, UK, Italy and the Netherlands. It is 0.3 – 0.35 for Israel, Austria, Japan, Germany; 0.1 for Sweden. The parameter  $c$ , the initial transmission rate, is 2.2 for the USA, 2.4 for UK, Austria, Sweden, the Netherlands, 2.6 for Israel, Italy, Germany, Japan; it reaches 4.5 – 5.5 for Brazil and India (with  $a < 0.05$ ). Here  $c$  can be mostly ”captured” during the early stages;  $a$  became ”reliable” later, when the management the epidemic reached some stability.

**Covid-19 in UK.** The coincidence of the *red dots* with our  $u(t)$  for the USA could be because this was an average over 50 states. Let us consider UK for the period from March 16 till April 15; see Figure 3.

Then  $c = 2.4, a = 0.2$ ; the scaling coefficient is 2.2. The total number of cases will be now divided by  $10K$ , not by  $100K$  as for the USA. The increase of  $c$  to  $c = 2.4$  qualitatively indicates that the ”response” of the population to *Covid-19* was a bit weaker in UK than in the USA

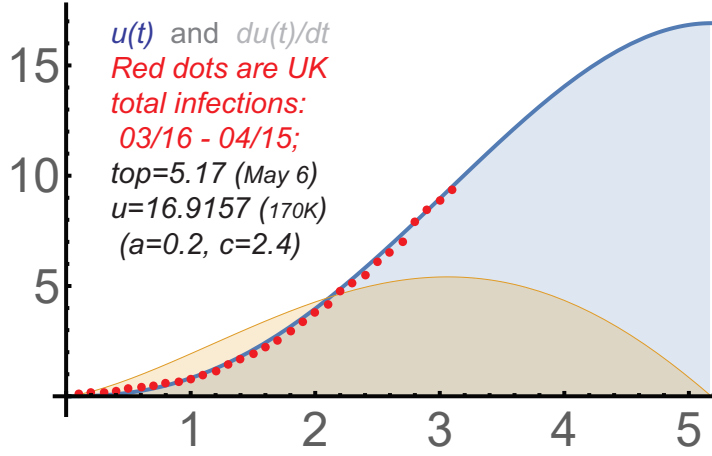


FIGURE 3.  $u(t) = 2.2 t^{(c+1)/2} J_{(c-1)/2}(\sqrt{at})$  for  $c = 2.4, a = 0.2$

for this period, and/or the regular number of contacts was somewhat greater. Though this is really some little change.

Recall that if the spread of disease is not *actively* managed, then the growth  $\approx t^c$  can be expected, so  $c$  reflects the strength of the virus and how we, especially the infected people and those who think that they are infected, react to the numbers of infections *before* the active management begins. Providing the numbers of infections, discussing them by the authorities and in the media are some management too, but *passive*. By "active", we mean the modes (A), (B) in this work.

The estimate for the "saturation moment" was 5.17, i.e. about 51 days after March 16, somewhere around May 6 with the corresponding number of infections about 170000, assuming that the "hard" measures would continue as before April 15. The latter did not materialize.

**Austria: 3/07-4/15.** This is one of the earliest examples of a complete phase 1. There is some switch to a linear growth around and after the "saturation", typical in all countries that reached the saturation. Modeling this period by Bessel function appeared quite doable, so the management was steady and of type (A). See Figure 4.

Here we start with March 07; Austria began earlier with the protection measures than UK and the USA. The parameters  $a = 0.33, c = 2.4$  and the scaling coefficient 3 appeared the best for Austria; we divide now the number of infections by 1000, i.e. 14 in the graph corresponds to 14000 infections.

**Switzerland: different stages.** We focus on the period March 13- April 12. As we have already discussed, (A) is supposed to dominate closer to the turning point and then toward  $t_{top}$ . Mode (B) is present too, but we mostly see in the figures the result of "hard" measures.

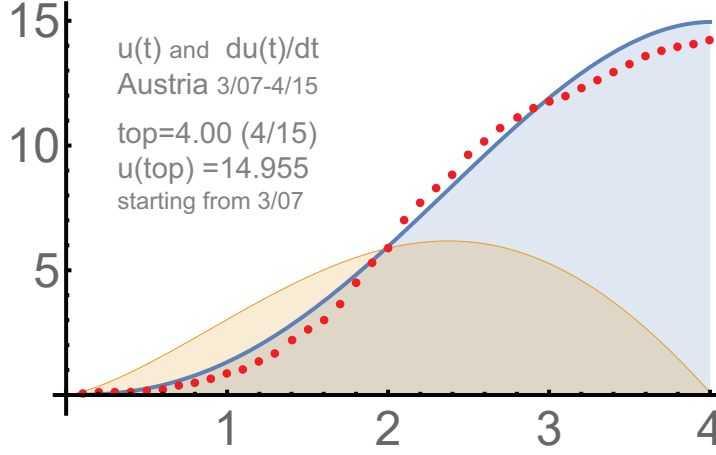


FIGURE 4.  $u(t) = 3t^{(c+1)/2} J_{(c-1)/2}(\sqrt{at})$  for  $c=2.4, a=1/3$

Recall that only the total number of the detected infections is considered in this paper. The starting moment is  $t = 0$ . This is when the intensive growth of power type begins, and also the beginning of active management. It was around March 12 in Switzerland in Figure 5. The first results of the employed measures can be seen around March 20 : a transition of the initial (mostly) parabolic growth to the linear one.

Some "free" spread of quadratic-type is present in practically all countries in the early stages of *Covid-19*. Though in Brazil and India, the initial growth was higher:  $\sim t^{4.5}$  and  $\sim t^{5.5}$ . The usage of Bessel functions continuously (and automatically) diminishes the exponent here during phase 1.

This is different for mode (B): the transition from the "free" growth  $u(t) \sim t^c$  to  $u(t) \sim t^{c/2} \cos(\dots)$  is due to the increase of  $a$  from 0 to  $a > c^2/4$ ; then the exponent will stabilize even if  $a$  continues to increase. Phase 2 is with  $a > c^2/4$ ; The role of  $\cos(\dots)$  and  $\sin(\dots)$  in (9) becomes significant and provides the "final saturation": the technical end of the 2nd phase (and the 1st wave).

Let us briefly comment here on changing the starting point from the absolute start of the epidemic to some  $t_\bullet$ . The equations will remain the same, but  $c/t$  must be replaced by  $c_\bullet/(t - t_\bullet)$  for the current  $c_\bullet$ . There can be different stages of epidemics, so this can be necessary. Such a split of the total investment period into intervals treated independently is very common in stock markets. However, we do not change the starting point  $t = 0$  when switching from phase 1 to phase 2. The corresponding (B)-type solution is considered as started from the very beginning (though it is used only around and after  $t_{top}$  for mode (A)).

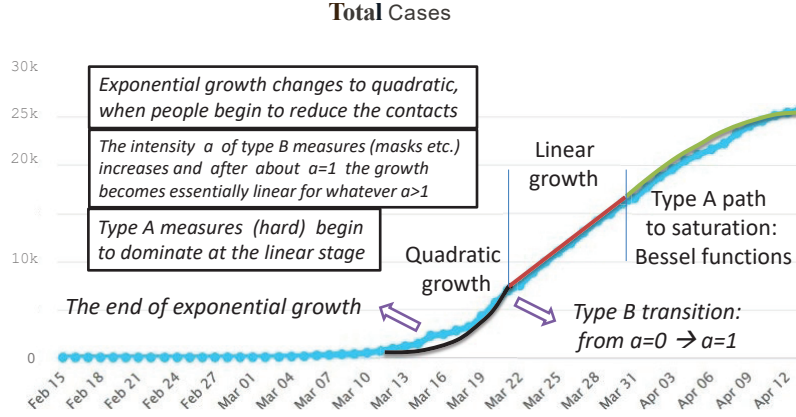


FIGURE 5. Covid-19 in Switzerland

**9. Main findings.** The "power law of epidemics" presented as a differential (initially, difference) equation is the starting point of our approach to momentum management. This law is different from other power laws for infectious diseases; compare e.g. with [MH]. We deduce it from certain "geometric" assumptions concerning the contacts of infected people, a sort of principle of local herd immunity, and from some behavioral and sociological analysis. The restrictions people impose themselves during the epidemic, mostly the reduction of their contacts are related to the general theory of "momentum risk-taking" from [Ch1].

The main problem here is to "couple" the *power law of epidemics* with some mechanisms for their ending. These are major challenges, biologically, psychologically, sociologically and mathematically. We demonstrate that mathematically there is a path: Bessel functions serve as a natural way from the power law of epidemics to the "saturation". Our differential equations are based on various simplifications; however their match with the real data appeared almost perfect.

The "megaproblem" of understanding and managing epidemics is ramified and interdisciplinary; significant assumptions are inevitable in any models. We model only the period when the total number of infections is significantly smaller than the whole population. We also disregard the recovery and quarantines, though they are indirectly incorporated in our differential equations via  $c$  and  $a$ .

We are fully aware of the statistical nature of the problem. The usage of random processes, like *Bessel processes*, is reasonable here to address the randomness around epidemics; see the end of Section 7. Some combination with the traditional SIR model can be possible too; see e.g. [CLL]. Our equations have natural "logistic" extensions.

**Saturation via hard measures.** The main outcome of our modeling and this paper is that the measures of "hard type", like detecting infected people, followed by their isolation, and closing the places where the spread is likely, are the key for ending an epidemic. Such measures are a must for at least the initial and middle stages of the epidemic to ensure the saturation in our approach.

Moreover, they must be employed strictly proportionally to the current number of infections, not its derivative of any kind, to be really efficient. This is the most aggressive way to react, which we call mode (A) in the paper. This can be seen in many countries, at least during the middle stages of the epidemic.

Then the point  $t_{top}$  of the first maximum of the corresponding Bessel function times  $t^{c/2+1/2}$  is a good estimate for the duration of phase 1; it also gives some projection for the expected maximum of the number of infections during phase 1. This is assuming "hard measures" and steady management of type (A). This formula worked very well for middle periods almost everywhere and even for the *whole* period of the extensive spread in the countries and areas that reached phase 2. It seems a real discovery.

If the saturation is successfully reached at  $t_{top}$ , then the *second phase* begins, which is essentially the switch to mode (B). Mathematically, the curve of total cases significantly changes around  $t_{top}$ . This switch can be clearly seen in many countries: frequently, a well-visible break of the derivative.

The second phase is more challenging mathematically; it is heavily influenced by economic, political and other factors. So it is even more surprising, that it can be modeled with high accuracy using our system of differential equations of type (B). See our graphs for Israel, Italy, Germany, Japan, and the Netherlands in Section 11.

The quasi-periodicity of our  $u$ -functions under momentum management of type (A) and that under (B) in terms of  $\log(t)$  is the key mathematical reason for reaching the saturation in our approach. This is not connected at all with the periodicity of epidemics associated with seasonal factors, biological reasons, or various delays; see e.g. [HL]. The saturation we model entirely results from the active management and general "response" of the population to the threat. *Covid-19* is exceptional in many ways, the scale and the intensity of the measures used to suppress it are quite unique. The *second wave*, which can be



now observed in several countries, the USA, Israel, Japan, several in Europe, and more of them, is a clear confirmation of the leading role of hard measures. It really looks like the main "control parameter" is their intensity.

With this reservation about the source of our "periodicity", there is some analogy with *Farr's law of epidemics*. Under mode (A), this is some reflection symmetry of  $du(t)/dt$  for  $u(t) = t^{c/2+1/2} J_{(c-1)/2}(\sqrt{at})$  in the range from  $t = 0$  to  $t_{top}$ , the first local maximum of  $u(t)$ . The portions of the corresponding graph before and after the *turning point* are not exactly symmetric to each other, but are close enough to this. See e.g. Figure 1, where the turning point is at  $\max\{du(t)/dt\}$ . This holds for  $w(t)$ , describing the (AB)-mode, but the second "half" becomes somewhat longer than the first. This is for the first phase.

**The second phase.** Mode (B) is the usage of the average  $u(t)/t$  instead of  $u(t)$  and relying mostly on "soft" measures, like wearing protective masks and social distancing. Closing schools is certainly a hard measure by any standards, and a very important one. Some travel restrictions are "hard" too. Self-imposed limitations are of course important too, and can be quite hard. They can significantly complement the governmental management, as occurred many times in the history of epidemics.

When used alone, soft measures are generally insufficient to "reach zero", which follows mathematically from our model. However, the usage of "hard measures" combined with the response based on  $u(t)/t$  instead of  $u(t)$  can work reasonably quickly toward the saturation; this is mode (AB).

The best way to address the late stages appeared our "two-phase solution". Since the hard measures are reduced or even abandoned at the end of phase 1 (or even before), we switch from mode (A) to (B). This can be seen in quite a few countries that reached the "saturation". There is a clear linear-type pattern around the "technical saturation", which is  $t_{top}$ , the point of maximum of our Bessel-type  $u(t)$ . Then the total number of detected infections closely follows  $Ct^{c/2} \cos(d \log(t))$  for some  $C$  and  $d = \sqrt{-D}$  from (7),(9). Here  $c$  is the exponent of the initial power growth of  $u(t)$ ; it remains the same for any modes, (A), (B) or (AB). As for  $d$ , it must be adjusted numerically to match the shape of the curve of the actual number of total cases near and after the saturation;  $C$  is a (constant) rescaling coefficient.

This formula describes the late stages with surprising accuracy in almost all countries that entered phase 2; there are already quite a few, for instance, almost all Western Europe by now. The usage of our *two-phase solution* is less relevant for the countries that begin reducing

or abandoning hard measures upon the first signs of the stabilization of new daily cases or implement hard measures insufficiently. This includes some countries, as UK and the USA, with solid type (A) response during the initial and middle stages. See Section 10; the USA (as the whole) did not reach the end of phase 1 before switching to the second wave.

If the period of linear growth becomes long, then  $d$  in  $\cos(d \log(t))$  can be more difficult to find. Such long periods of linear growth of the total number of detected infections were typical for the countries that do not employ "hard" measures systematically, like Sweden. These measures are present in some forms anywhere, but this can be insufficient. The growth of the number of total cases can be significantly faster than linear for sufficiently long periods, which can be due to a variety of factors, including insufficient detection-isolation capacities and some general weakness of the health-care systems; Brazil and India are examples.

**The risks of recurrence.** The recurrence of epidemics is a clear challenge for microbiology, epidemiology and population genetics; very much depends on the type of virus. The "natural"  $c$ -coefficient reflects both, the transmission strength of the virus and the "normal" intensity of our contacts. The second component is likely to return back to normal after the epidemic is considered "almost finished". If the "microbiological component" remains essentially the same as it was before, the recurrence of the epidemic is almost inevitable after the protection measures are removed. The recurrence of the epidemic becomes a sort of "cost" of our aggressive interference in its natural course.

The whole purpose of aggressive management, mode (A) in our approach, is to keep daily new case at reasonably small levels. Then *detection-isolation-tracing* becomes much simpler and the pressure on medical facilities reduces. However the "saturation" in one place is of course not the end of the epidemic. New clusters of infections are likely to emerge, and the epidemic suppressed in one area can still continue in other places.

These are real risks. The economic and other "costs" of hard measures are very high. It is understandably easy to "forget" that the turning point and the saturation were achieved reasonably quickly mostly due to the hard measures imposed. The corresponding underlying mathematical processes have a strong tendency to become periodic, which can "play against us" as we approach the end of the epidemic.

Unless the *herd immunity* is reached or the virus lost its strength, "restarting" the epidemic with few infected individuals left after the previous cycle is standard. Significant numbers of those recovered and

the asymptomatic cases provide some protection, but it can be insufficient. For the next cycle(s), our better preparedness can be expected, which can diminish  $c$ . However this is not confirmed so far in the countries with 2nd waves; there are obvious problems with restarting hard measure, including keeping schools close.

Finally, let us emphasize that our differential equations describe an *optimal* momentum response aimed at diminishing the new infections only under the following key condition. We assume that people and the authorities in charge *constantly* monitor the numbers of infections and momentarily respond to them in the "most aggressive" way.

This is actually similar to the ways stock markets work. Professional traders simply cannot afford *not* to react to any news and any change of the stock prices, even if they seem random, temporary or insignificant. Indeed, any particular event or a change of the share-price can be a beginning of a new trend. Applying this to managing epidemics, we are really supposed to closely follow the data. The "flexibility" here is only the usage of some average numbers as the triggers, as a "protection" against random fluctuations. This is exactly mode (A) versus "more defensive" (B) or (AB).

**The table: (A) vs. (B).** For convenience of the readers, let us provide a basic table presenting the (A)-mode and the (B)-mode with some simplifications. This is Figure 6. Recall that  $c$  is the initial transmission rate,  $a$  the control parameter, which is the intensity of the management,  $\kappa$  the efficiency of protective masks.

By "Detections", we mean the total number of detected individuals till  $t$ , which is essentially proportional to the number of tests performed. This is up to "us" to control.

The response of type (A) is basically as follows: if the number of infections doubles, then the *rate of increase* of tests must be doubled, not just the number of tests. For (B), the rate of change of the measures is assumed proportional to the rate of change of the infections. The (AB) mode uses this kind of response for hard measures. So under (AB), if the number of infections doubles, then the number of tests must be doubled too.

This kind of response will provide the quasi-periodicity with respect to  $\sqrt{t}$ , so the saturation will take longer than under (A), where the quasi-periodicity is for  $t$ . However, the time till saturation under (AB) (roughly, 1/4th of the period) is generally "quite acceptable". See Section 10 below and Sections 4, 5.

Recall that the key hard measure is *testing & detection & isolation*, followed by *tracing*. Also, we use *only* the total numbers of detected infections, without "subtracting" the closed cases.

$U(t)$ : <i>total # of all infections till moment "t"</i>	CONTROL	GROWTH	ENDING
Natural Course: no active (gov) management	None, though "c" diminishes over time "t"	Firstly, $t^c$ for initial $c \approx 2$ and then later $c \rightarrow 1$	Due to virus mutations, ... , herd immunity
Under type A: the detection and isolation	t-derivative of <i>Detections</i> is $a U(t)$ , $t > 0$	$t^{\frac{c+1}{2}} J_{\frac{c-1}{2}}(t\sqrt{a})$ $\sim t^{c/2} \cos(t\sqrt{a})$	Approximately after $\pi / (2\sqrt{a})$ for intensity $a$
Under type B: masks, social distancing etc.	t-derivative of <i>(Masks used)</i> = $a U(t)/kct$	$t^{\frac{c}{2}} \cos(d \log t)$ $d = \sqrt{a - c^2/4}$	No fast ending due to $\log(t)$ - "periodicity"

FIGURE 6. Two types of momentum management

Switching to (B) in the table, by "Masks used", we mean the total number of infected people who began using the masks till  $t$ . If the number of infections doubles, than the total number of masks must be doubled too under (B), *not the rate of change* as for (A).

**10. Unusual patterns.** Our key finding is that the *total* numbers of detected infections for *Covid-19* can be described with high accuracy by  $u(t) = C t^{c/2+1/2} J_{c/2-1/2}(\sqrt{a}t)$  during the initial and middle stages of phase 1, which was practically in all countries we considered. This is the period of intensive growth of the spread when the hard measures are coupled with the most aggressive response to the changes of the numbers of total cases. A typical example is Figure 1.

It appeared that the whole phase 1 was covered well by such functions if the (A)-mode was employed until the numbers of new detected infections dropped to really small levels. South Korea, Austria, Israel, Italy, Germany, Japan, the Netherlands and many other countries (almost all Western Europe) did exactly this. Then  $t_{top}$ , the first zero of  $du(t)/dt$ , is a reasonable estimate for the "technical end" of phase 1.

To understand the usage of type (A) curves for forecasting, we determine the parameters  $a, c, C$  for the initial periods, the *red dots*, and then analyze sufficiently long test periods, the *black dots*, without changing  $a, c, C$ . A challenge here is the usage of  $a, c, C$  obtained in some *early* stages for forecasting the later ones.

This seems doable, if the hard measures are employed, and when the management is steady, which was not (always) the case with Sweden, USA, UK and some other countries. There were significant periods of essentially linear growth of the curves of total (detected) cases in these countries. In our charts, the *black dots* remained essentially linear significantly longer than it was "allowed" by the corresponding Bessel-type  $u(t)$ , based on the parameters obtained at earlier stages. In the USA, the process appeared the most complicated from these 3 countries. Brazil and India also must be considered exceptional because their  $c$ -coefficient are exceptionally high. By now (August 25), they are still in the middle half of phase 1.

We note that the parameters  $a, c$  were the same for the Netherlands and UK, and not too different for those for the USA. However, the Netherlands reached phase 2 following the  $u$ -curve, as well as many countries in Western Europe. So this was not about the values of the parameters, but rather about significant changes with the management of *Covid-19* in the USA and UK.

One can expect the (AB)-mode to occur after the mode (A) is "relaxed". Actually, the moments of the change of the management can be clearly seen in the graphs for the USA and UK. We found the corresponding  $w(t)$  curves of type (AB) matching the *red dots* and *black dots* till these moments for these countries. We also calculated the  $w$ -curves for Israel and Sweden, some "control group";  $w(t)$  is not needed for Israel, which reached  $t_{top}$  under our  $u(t)$ , and the actual curve of total cases for Sweden was not supposed to match  $u(t)$  or  $w(t)$ .

Recall that mode (AB) is when the hard measures are still present, but the response to the total number of infections becomes softer, as under (B). For instance, if the number of new cases is essentially a constant, even uncomfortably high, the testing-detection under the (AB) will be essentially constant too. This is much more aggressive with (A). Considering the (AB) mode is not necessary for the countries that reached  $t_{top}$  under (A). For such countries, the passage will be from (A) directly to mode (B), to the *second phase*.

The *blue dots* till 05/27 after the *black dots* were added to monitor the usage of the  $w(t)$ -functions. They did not stay within  $w(t)$  for Sweden and the USA, This was expected for Sweden, since no aggressive approach was implemented there at that time. For the USA, there was another significant reduction of hard measures. UK "managed" to

stay within the *forecast cone* between  $u$  and  $w$ ; its "expiration" was June 10. Then it entered phase 2, and the curve of total cases matched well our "2-phase solution". Sweden eventually reached phase 2 too, but this occurred significantly later.

When using  $w(t)$ , the point  $t_{top}^w$ , the (first) maximum of  $w(t)$ , is a reasonable upper bound for the "technical saturation". The prior  $t_{top}^u = t_{top}$  then is a lower bound; we obtain some forecast cone.

Let  $u(t) = Ct^{\frac{c+1}{2}} J_{(c-1)/2}(t\sqrt{a})$ ,  $w(t) = Dt^{\frac{c+1}{2}} J_{c-1}(2\sqrt{tb})$ . Using (18), the match  $u(t) \approx w(t)$  near  $t = 0$  gives:

$$(21) \quad \frac{C}{D} \approx \left( \frac{2b}{\sqrt{a}} \right)^{\frac{c-1}{2}} \frac{\Gamma((c+1)/2)}{\Gamma(c)} \quad \text{for the } \Gamma\text{-function.}$$

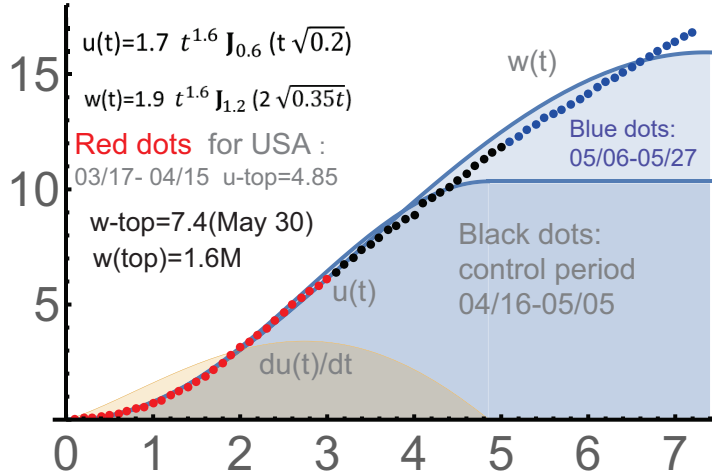


FIGURE 7. USA:  $c=2.2$ ,  $a=0.2$ ,  $C=1.7$ ;  $b=0.35$ ,  $D=1.9$ .

The cone for the USA. The prior  $t_{top} = t_{top}^u$  for  $u(t)$  was May 5, with  $a, c, C$  calculated on the bases of the data till April 16, marked by *red dots*. It was under the expectations that the "hard" measures would be applied as in (A), i.e. as before April 16. The *black dots* represent the control period. The challenge was to understand how far  $u(t)$  can be used toward the "later stages". The match was very good for quite a long period of time (the same with UK), but then the curve went up, which we mostly attribute to the softening the management mode, namely, relaxing hard measures. The "response" of the population of the USA to the threat noticeably softened too.

Whatever the reasons, the switch to  $w(t)$ , describing the (AB)-mode, appeared necessary. The trend was initially toward  $w(t)$  for the USA,

but then the *blue dots* "went through"  $w(t)$ . Generally, the test dots can be expected to stay within the *forecast cone*, subject to standard reservations: the usage of hard measures and steady management. The cone was the domain between  $u(t)$  extended by a constant  $u(t_{top})$  for  $t > t_{top}^u$  and the graph of  $w(u)$  till  $t_{top}^w$ , which was approximately May 30, 2020.

The parameters  $b, D$  of  $w(t)$  were calculated to ensure good match with *red dots*;  $c$ , the initial transmission rate, is *always* the same for  $u(t)$  and  $w(t)$ . The graphs of  $u(t)$  and  $w(t)$  are very close to each other in the range of *red dots*. The above relation for  $C/D$  holds with the accuracy about 20%.

The  $w$ -saturation value was around 1.6M, but mostly we monitor the *trend*, the "derivative" of the graph of black dots, which is supposed to be close to the derivative of  $w(t)$  or  $u(t)$ . See Figure 7. Some spikes with number of cases are inevitable; it is acceptable if the dots continue to be mainly "parallel" to  $u(t)$  or  $w(t)$  (or in between).

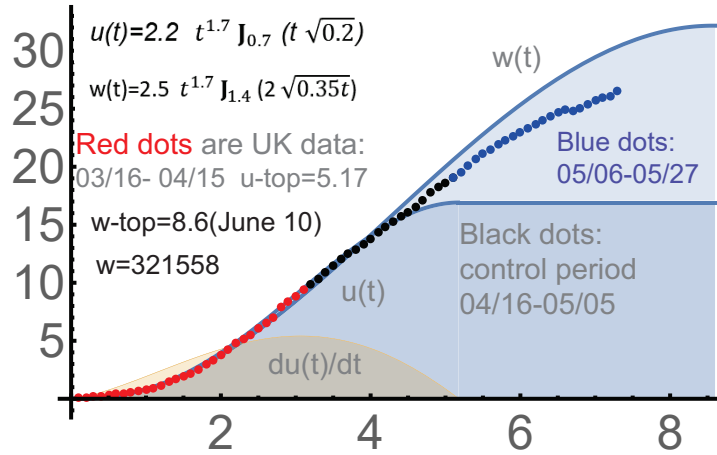


FIGURE 8. UK:  $c=2.4, a=0.2, C=2.2; b=0.35, D=2.5$ .

UK till June 10. The graphs of  $u(t), w(t)$  with prior red-black dots and the blue ones added after May 5 are in Figure 8. The expected  $t_{top}^w$  was around June 10. The total number of detected infections was expected 330K or below. These "predictions" of course depended on many unknown factors. However, some argument in favor of the stability of our model is that any spikes with the numbers of infections are supposed to trigger additional actions of the authorities in charge and increase our own protective measures. Such "self-balancing" seems a rationale for relatively uniform patterns of the spread of *Covid-19* in different countries.

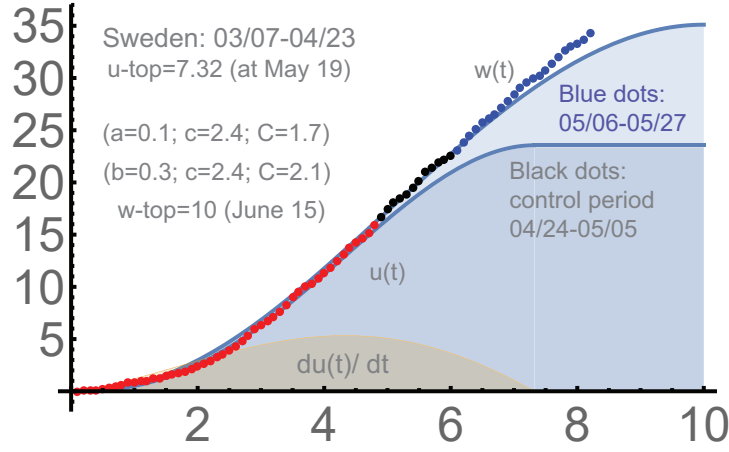


FIGURE 9.  $w(t) = 2.1t^{(c+1)/2}J_{c-1}(2\sqrt{bt})$ ;  $b=0.3$ ,  $c=2.4$ .

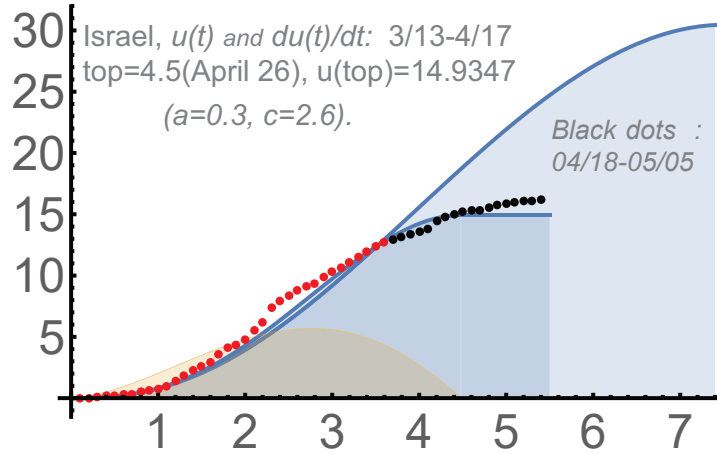


FIGURE 10.  $u(t) = 2.2t^{(c+1)/2}J_{(c-1)/2}(\sqrt{at})$ ,  $c=2.6$ ,  $a=0.3$ .

**Sweden: anti-forecast.** Sweden is actually expected *not* to follow our  $u(t)$  and  $w(t)$ ; this country did not follow hard ways with fighting *Covid-19*. We calculated  $w(t)$  to confirm this; see Figure 9. Its expiration was approximately after 100 days ( $x = 10$ ); i.e. the  $w$ -saturation was about June 15. We did not expect this saturation to occur. Definitely some measure were in place in Sweden; for instance, people readily contact the authorities with any symptoms of *Covid-19*. However this did not change much the linear growth of the spread until recently, when the country really did something to reduce the spread (and the vacation period helped).



**Israel:**  $u(t)$  worked. Here the usage of  $u(t)$  was sufficient to model the total number of detected cases till the "saturation", which occurred almost exactly when  $u(t)$  reached its maximum. The black dots demonstrate well the "linear period" after the saturation, which was essentially of the same type as in South Korea, Austria and quite a few countries that went through the saturation. Nevertheless, we provide the *forecast cone* calculated as above on the basis of  $w(t)$ . In contrast to the USA, UK and, especially, Sweden, the black dots are much closer to the flat line started at the  $u$ -top, which was at  $t = 4.5$  (April 26).

**Brazil:** 3/29-8/23. This is an ongoing process with high  $c$  and low  $a$ . The initial parameters were determined for the *red dots*: from 3/29-6/22 with the starting number 3904 of the total cases. The black dots (the testing period) were till 8/23, 2020. See Figure 11.

Their parameters are  $a = 0.04, c = 4.47, C = 0.65$ , where we set  $y = \text{cases}/10K$ . In contrast to the previous examples, we use  $u_1 = Cu^1$  and the second (non-dominant) solution  $u_2 = Cu^2$ :

$$u(t) = u_1(t) - 0.35u_2 = Ct^{c/2+0.5} (J_{c/2-0.5}(\sqrt{at}) - 0.35J_{0.5-c/2}(\sqrt{at})).$$

The cone will not be provided, since the curve of real detected cases is still within our  $u$ -curve. Note that the parameter  $a$ , the intensity of "hard measures", is very low, and  $c$  is quite large.

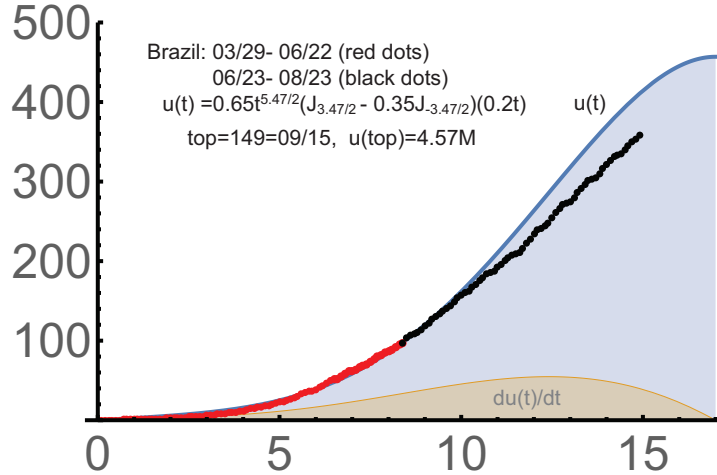


FIGURE 11. Brazil:  $c=4.47, a=0.04, C=0.65$ .

**India.** The parameters are even more extreme for India:  $a = 0.035, c = 5.2$ . This country is still in the period of polynomial growth of the spread, as of August 25. The analysis of India is obviously important to understand the future of *Covid-19*. We provide the corresponding

$u$ -curve. Recall that it is under the assumption that the "hard" measures are used in a steady manner, which was the case in almost all Western Europe, China, South Korea, the USA (during some periods), and in several other countries. Also, a sufficiently high level of health-care system and the uniformity of measures in the whole country are necessary for the success of such measures.

Even when all these factors are present, the spread can be very intensive. This occurred in the USA, where the  $u$ -curve and  $w$ -curve served well only the middle stages. In India, the parameters of the spread were the most extreme among the countries we consider in this paper:

$$u(t) = C t^{c/2+0.5} (J_{c/2-0.5}(\sqrt{at}) + 0.2 J_{0.5-c/2}(\sqrt{at})), c = 5.2, a = 0.035.$$

We set  $y = \text{cases}/10K$  in Fig. 12. The period we used to determine the parameters was 3/20-8/23 (no "black dots"). The starting number of detected cases was 191, which was subtracted,

Actually,  $0.0125(t+0.07)^{3.65}$  gives a good approximation for the main part of the period; see Figure 12, where the graph of this function is shown as brown. So this is really a period of (strong) polynomial growth, but *obviously* not of any exponential growth. We never observed exponential growth of the number of detected infections with *Covid-19* beyond some very short initial periods.

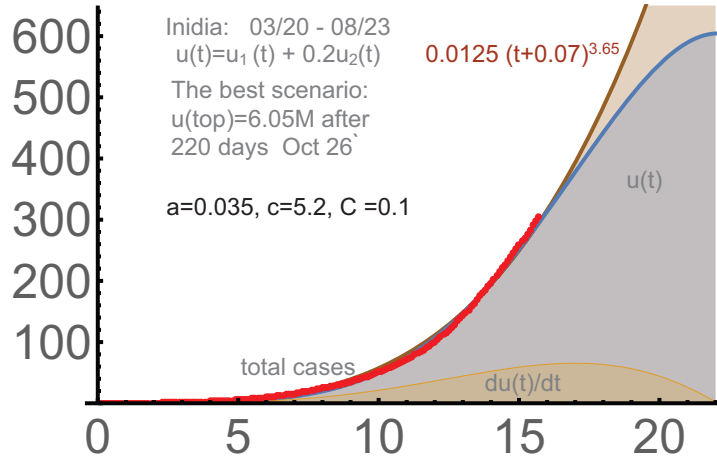


FIGURE 12. India : 3/20 – 8/23,  $c = 5.2$ ,  $a = 0.035$ ,  $C = 0.1$ .

**11. Two-phase solution.** Let us describe our *two-phase* model for the total number of infections. It is from the beginning of the intensive growth of cases through the saturation  $t_{top}$  of the (A)-phase, and from  $t_{top}$  till the "final saturation" of the corresponding (B)-phase. It

works surprisingly well for the countries that managed to reach reasonably small numbers of new daily infections during the first phase; the "forecast cone" and the  $(AB)$ -mode appeared unnecessary for them.

We determined below the parameters  $a, c, d$ , and the scaling coefficient  $C$  for the period till May 22 (2020). So all dots are red unless for Israel, where we used  $a, c, C$  above found in the middle of April. The epidemic is of course far from over, but the first "wave" ended in these countries; so no test periods, "black dots", were considered.

Recall that the parameters  $a, c, C$  are mostly obtained to ensure the match for the intervals till the "turning points";  $d$  can be determined only in the vicinity of  $t_{top}$ , if it is reached. The initial transmission rate  $c$ , must be the same for  $(A)$  and  $(B)$  according to our theory.

The leading solution from (7) is  $u_B(t) = C_B t^{c/2} \cos(d \log(Max(1, t)))$ , where  $c$  is the one in  $u(t) = C_A t^{(c+1)/2} J_{(c-1)/2}(\sqrt{a}t)$ ,  $d = \sqrt{a_B - c^2/4}$ . The scaling coefficient  $C_A, C_B$  are adjusted independently; the intensity parameters  $a = a_A$  and  $a_B$  have different meanings too. In the later stages, we assume that  $a_B > c^2/4$ . Here  $Max(1, t)$  is due to some ambiguity at  $t = 0$ ; anyway, we use  $u_B(t)$  only for  $t > 1$ . Here  $d$  equals very approximately to  $\sqrt{a}$  for considered countries.

Importantly, we start  $u_B(t)$  at  $t = 0$ , though it is used only after or around  $t_{top}$ . This results in the following nice formula for the end  $t_{end}$  of phase two:  $t_{end} = \exp(\frac{1}{d} \tan^{-1}(\frac{c}{2d}))$ .

Israel: 03/13-05/22. We already closely considered the first phase:  $u(t) = 2.2 t^{(c+1)/2} J_{(c-1)/2}(\sqrt{a}t)$ , till  $t_{top}$  for  $c = 2.6, a = 0.3$ . For the second phase,  $d = 0.6$  and  $C_B = 3.4$ .

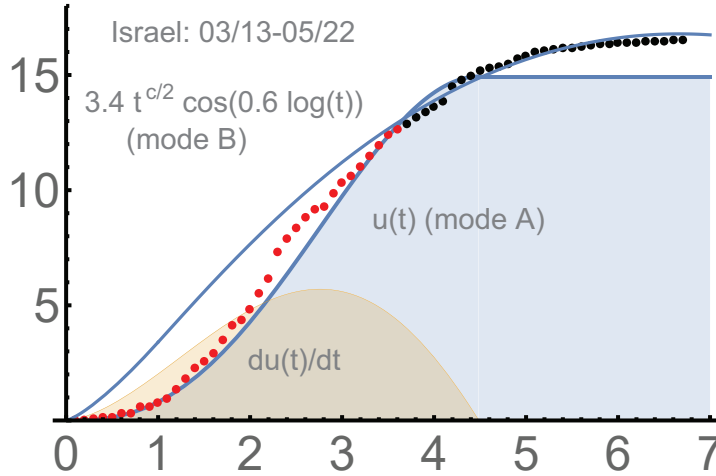


FIGURE 13. Israel:  $c=2.6, a=0.3, d=0.6$ .

Italy: 2/22-5/22. See Figure 14. The starting point was 2/22, when the total number of infections was 17; in this paper, we always subtract this initial value when calculating our *dots*. One has:

$$u_{1,2}(t) = 0.8 t^{(c+1)/2} J_{\pm \frac{c-1}{2}}(\sqrt{at}), \quad u(t) = u_1(t) - u_2(t), \quad \text{and} \\ u_B(t) = 2.85 t^{c/2} \cos(d \log(\text{Max}(1, t))), \quad c=2.6, a=0.2, d=0.5.$$

We use here the second solution  $u^2(t)$  from (14). For  $t \approx 0$ , it is approximately  $\sim t$ , i.e. smaller than  $\sim t^c$  for the dominating solution  $u^1$ . The top of the bulge occurs when  $u^2(t)$  reaches its minimum; which is approximately at  $t_{top}/2$ , where  $t_{top}$  is that for  $u_1$ . Actually, we can see similar bulges for Austria, Israel and in the Netherlands too, but they are relatively short-lived and  $u_1$  appeared sufficient. The linear combination  $u_1(t) - u_2(t)$  was found numerically; the coefficient of  $u_2$  is not always  $-1$ . Here and further in this section,  $u_1 = Cu^1$  and  $u_2 = Cu^2$  for  $u^{1,2}$  from (14) with the same rescaling coefficient  $C$ , found numerically.

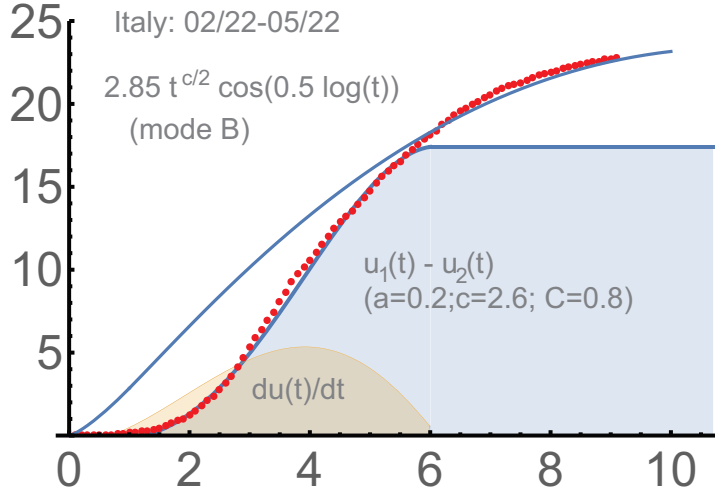
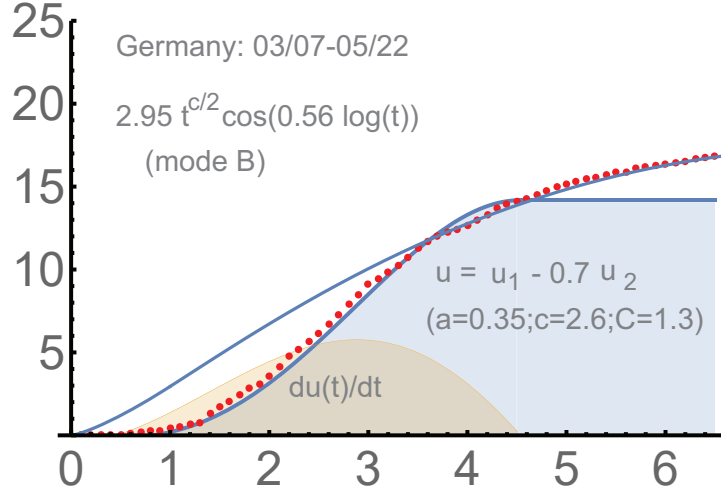


FIGURE 14. Italy:  $c=2.6, a=0.2, d=0.5$ .

Germany: 3/07-5/22. See Figure 15. We began here with the initial number of total infections 684, which must be subtracted when calculating the *red dots*. This was the moment when the curve began to look stable, i.e. a systematic management began. One has:

$$u_{1,2}(t) = 1.3 t^{(c+1)/2} J_{\pm \frac{c-1}{2}}(\sqrt{at}), \quad u(t) = u_1(t) - 0.7u_2(t), \quad \text{and} \\ u_B(t) = 2.95 t^{c/2} \cos(d \log(\text{Max}(1, t))), \quad c=2.6, a=0.35, d=0.56.$$

FIGURE 15. Germany:  $c=2.6, a=0.35, d=0.56$ .

It makes sense to provide the  $u$ -curve for the first phase in Germany using *only*  $u_1$ ; Figure 16. We disregard the bulge in the middle of *phase one*, which is actually similarly to what we did for Israel. The parameters are different:  $a = 0.2, c = 2.6, C = 1.7$ , i.e. now  $u(t) = 1.7t^{1.8}J_{0.8}(t\sqrt{0.2})$ .

For forecasting,  $u_1(t)$  seems the most reasonable to use regardless of the bulges. We "miss" the bulges, but then we mostly return to the curve calculated with  $u^2$ , similar to what we observed above with Israel. This remains essentially the same for Italy and Japan. Let us give the corresponding parameters for the usage of  $u = u_1$  only: Italy ( $c = 2.5, a = 0.1, C = 1$ ), Japan ( $c = 2.6, a = 0.1, C = 0.9$ ).

Practically, we always begin with using  $u^1$  only and obtain  $a, c, C$  for the interval before or around the turning point, when the bulge (if any) can be not really visible. Then they must be adjusted constantly, and  $u^2$  can be added if necessary. The initial  $a, c, C$  are of course subject to quite a few uncertainties.

Japan: 3/20- 5/22. See Figure 17. It was on top of some prior stage, so there were already 950 (total) infections on March 20. The curve is not too smooth, but manageable well by our *2-phase solution*:

$$u_{1,2}(t) = 1.5 t^{(c+1)/2} J_{\pm \frac{c-1}{2}}(\sqrt{at}), \quad u(t) = u_1(t) - 0.4u_2(t), \quad \text{and} \\ u_B(t) = 3.15 t^{c/2} \cos(d \log(\text{Max}(1, t))), \quad c=2.6, a=0.3, d=0.6.$$

The Netherlands: 03/13-5/22. Figure 18. The response to *Covid-19* was relatively late in the Netherlands; the number of the total case was

383 on 3/13, the beginning of the intensive spread from our perspective. A small "bulge" in the middle of the phase one can be seen here too, but  $u_1$  appeared sufficient: the country perfectly reached the saturation at  $t_{top}$  and then smoothly switched to phase two:

$$u(t) = 0.5 t^{(c+1)/2} J_{\frac{c-1}{2}}(\sqrt{at}), \quad c=2.4, \quad a=0.2,$$

$$u_B(t) = 0.86 t^{c/2} \cos(d \log(\text{Max}(1, t))), \quad d=0.54.$$

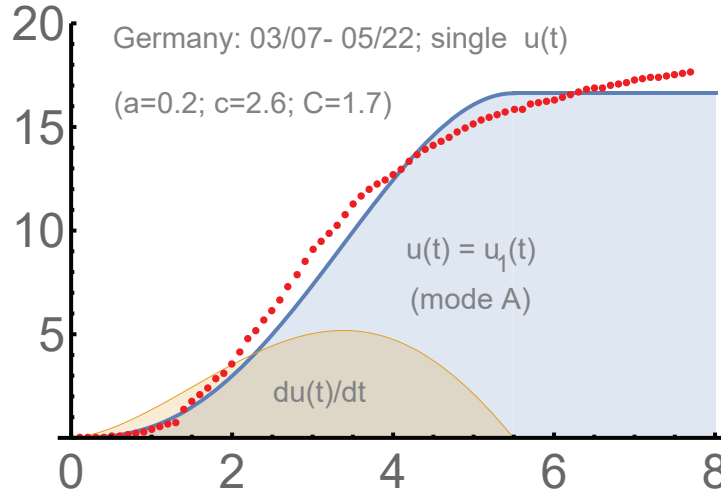


FIGURE 16. Germany:  $u = u_1 = 1.7t^{1.8}J_{0.8}(t\sqrt{0.2})$

To finalize, the best ways to use our curves for forecasting seem as follows:

- (1): determine  $a, c, C$  when the spread looks essentially linear;
- (2): update them constantly till the turning point and beyond;
- (3): expect the "bulges" to appear and add the  $u^2(t)$  if needed;
- (4): try to adjust the intensity of the measures to match  $u(t)$ ;
- (5): at the turning point, determine  $b, D$  and the bound  $w(t)$ ;
- (6): after the saturation at  $t_{top}$ , find  $d$  and switch to *phase 2*,

Generally, the data must be as uniform and "stable" as possible. Then underreporting the number of infections, the fact that these numbers mostly reflect symptomatic cases, and inevitable fluctuations with the data may not influence too much the applicability of the  $u, w$ -curves for phase 1, and  $u_B$  for phase 2. "Testing-detection-isolation-tracing" must be of course continued non-stop; the recurrence of the epidemic is a real threat.

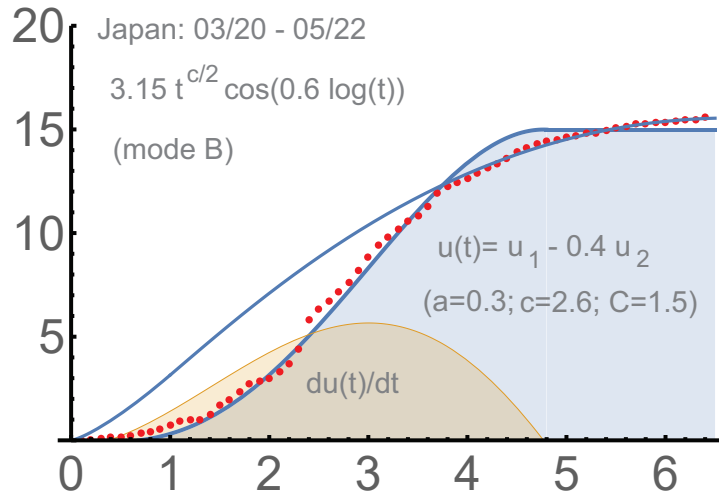


FIGURE 17. Japan:  $u = 1.5t^{1.8}(J_{0.8} - 0.4J_{-0.8})(t\sqrt{0.3})$ .

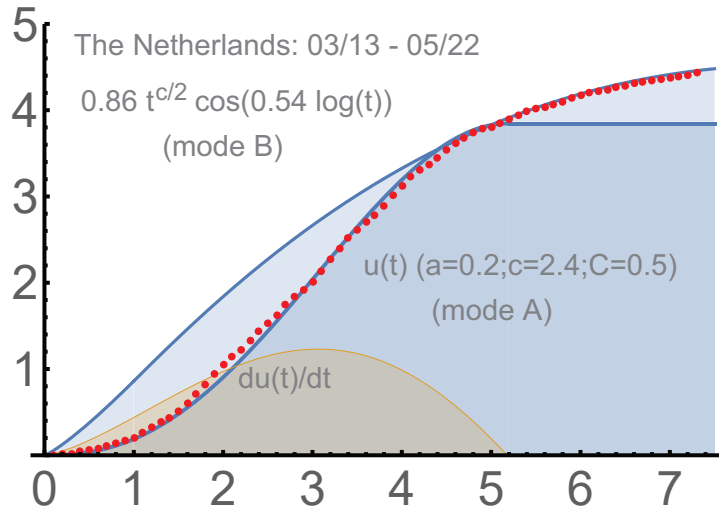


FIGURE 18. The Netherlands:  $u = 0.5t^{1.7}J_{0.7}(t\sqrt{0.2})$ .

**12. Entering second wave.** The second waves are supposed to occur (well) after the first ones. However this is not granted for *Covid-19*, where the spread heavily depends on active management. Efforts are needed to finish the first wave as quickly as possible to avoid building the second wave on the top of the first. So there must be reliable tools for forecasting during the second phase, which we actually have. Their importance is clear from the example of the USA.

As the whole, the country remained in phase 1, when the second wave began. However, there was a sufficiently long period when many states were actually in phase two. It was similar to Western Europe in July, but all major countries there were in phases 2 in contrast to the USA. However this appeared sufficient to predict the end of phase 2 in the USA around 09/19, which forecast was very stable for sufficiently long period. We used the following concept of "interaction".

Generally, all 50 states, must be considered separately; then the sum of the resulting curves is the forecast. However, such a straightforward approach does not take into consideration that improvements in one state positively impact the other ones. This is similar to stock markets. For instance, the components of *SP500* are supposed to be modeled individually, however their interaction must be taken into consideration.

The simplest approach to the interaction is what we actually used when taking the sums of two Bessel-type solutions,  $u_1$  and  $u_2$ . The second (non-dominating) can decrease as far as the total  $u(t)$ , a proper linear combination of  $u^1$  and  $u^2$ , increases. Similarly, the *superposition* of  $u$ -functions for different states or countries can be defined as their sum where "we allow" the components, modeling different states, to decrease as far as the total goes up. Here the physics intuition is relevant, but we will not specify.

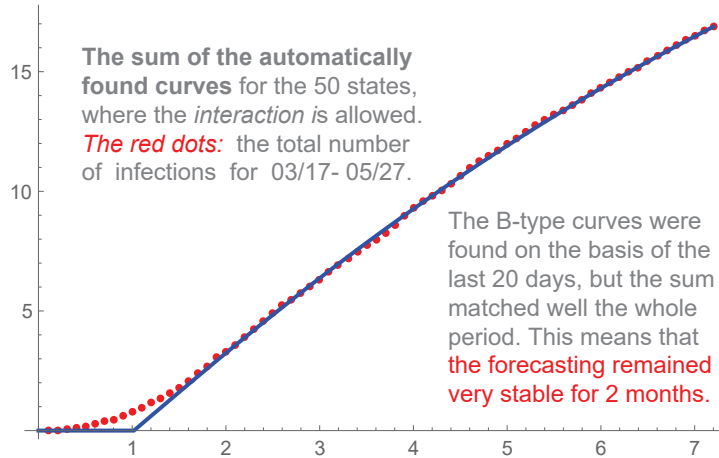


FIGURE 19. USA, the sum of the curves for individual states.

The corresponding analysis required a fully automated system, which was developed and will be made available. It produced the curves and determined the status of every state "without human interference".

The first automated forecast for 50 states was based on the period 03/17-05/27; we use for our forecasts for the USA the data from the



site <https://github.com/nytimes/covid-19-data>. Every state was processed individually. The *red dots* are the total numbers of detected cases, as above.

Our program focuses on the last 20 days; however, the match with the total number of detected infections appeared *perfect* almost from 03/17 and remained so for further auto-forecasts for a long period; see Figure 19. Such a high level of stability is actually rare in any forecasting, which made the chances to reach the saturation around 9/19 high. However, the hard measures were significantly reduced at the end of May practically in all 50 states. As a result, the number of states that reached phase 2 dropped from about 22 (at 5/27) to 8 (at 7/12). Then, in the second half of June the USA entered the *second wave*. We provide the automated output of our program from 6/21, one of the last before the curve of the total cases in the USA changed dramatically.

The "curve average" in this output is the maximum and the corresponding value of the average of 9 last curves  $u_B(t)$  for the USA, i.e. the moving average. The 9-day average is the simple average of the corresponding maxima; see Figure 20.

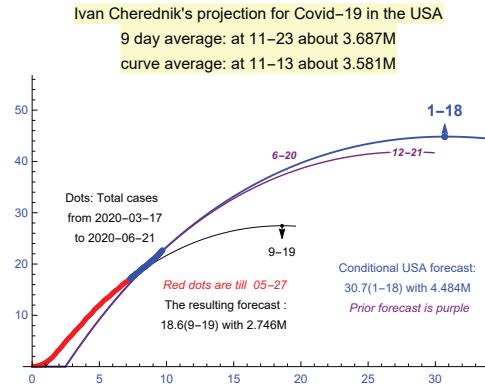


FIGURE 20. The forecast for the USA as of 6/21.

This is quite different from what our program gave for Europe *till the end of July*, to be exact for the following 45 countries: Albania, Andorra, Austria, Belgium, Bosnia and Herzegovina, Bulgaria, Croatia, Cyprus, Czech Republic, Denmark, Estonia, Faeroe Islands, Finland, France, Germany, Gibraltar, Greece, Guernsey, Hungary, Iceland, Ireland, Isle of Man, Italy, Jersey, Kosovo, Latvia, Liechtenstein, Lithuania, Luxembourg, Macedonia, Malta, Monaco, Montenegro, Netherlands, Norway, Poland, Portugal, Romania, San Marino, Serbia, Slovakia, Slovenia, Sweden, Switzerland, Vatican. See Figure 21.

As of July 8, the following countries had clear second waves: Albania, Bosnia and Herzegovina, Bulgaria, Croatia, Czech Republic, Greece, Kosovo, Luxembourg, Macedonia, Montenegro, Romania, Serbia, Slovakia, Slovenia. Sweden,

Poland, Portugal and some other countries did not reach phase 2 at that time. Nevertheless, the forecasts were sufficiently stable, though with a tendency to increase. Such stability changed this fall due to the end of the vacation periods and the beginning of the school year.

The saturation projections are of course of technical nature, certainly *not for the end of the spread*. By design, the "saturation targets" are supposed to increase over time. Moreover, a modest linear growth of the total number of detected infections is expected after the "saturation", if it was achieved.

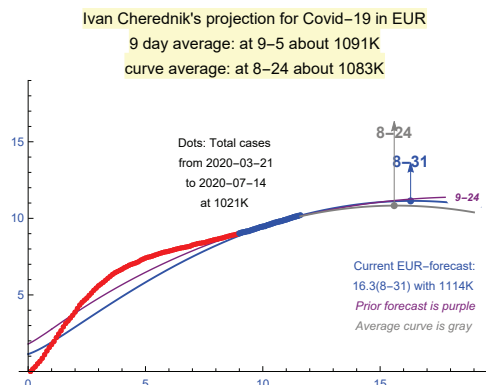


FIGURE 21. The forecast for Europe as of 7/14.

In Europe, the second phase was stable for quite a long period, but then the spread there changed significantly at the end of July, which is very similar to the beginning of the "hockey hook" in the USA shown in Figure 20. The saturation target in Figure 22 still exists, but it moved to December and is only of some symbolic value. Somewhat later, the 9-day average curves became essentially linear: the vacation period was over.

**Second waves.** We will focus on the second wave in Israel, where it appeared of unexpectedly large magnitude, and in the USA, where it began with a very large number of new daily cases due to the unfinished first wave. The expectations were that the parameter  $c_0$  for the 2nd wave could be essentially the same as  $c$  for the 1st. This was based on the assumption that the termination of the first wave was mostly due to the "hard measures". So if they are reduced or abandoned, the epidemic can be back with about the same parameters. It appeared actually worse than expected: the intensity of hard measures during the 2nd wave dropped significantly in Israel and the USA. It is not impossible though that some lower intensity of hard measures can have the same impact during the 2nd wave.

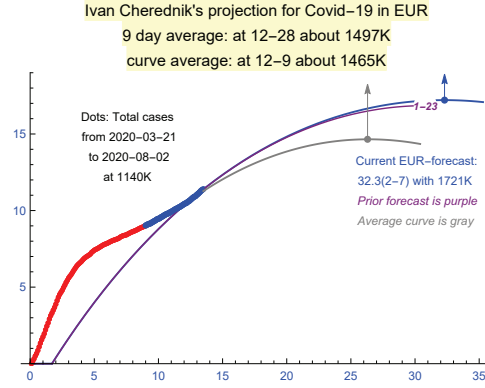


FIGURE 22. The forecast for Europe as of 8/02.

With Israel:  $c_o = 2.75$ ,  $a_o = 0.1$ ,  $C_o = 4.8$ , and the corresponding  $u_o(t) = C_o t^{c_o+1/2} (J_{c_o-1/2} + 0.1 J_{1.2-c_o}(\sqrt{a_o}t))$ ; the parameters were determined for the period 6/13- 7/14 and served well till about 07/30, when the change of the trend was similar to the transition from phase 1 to phase 2 we observed in quite a few countries. Then the number of cases began to increase dramatically.

The starting value at 06/13 was 18875, the number of cases at 7/7 was 31K. The black (control) dots were added at 7/14. See Figure 23;  $y = \text{days}/1K$ . The parameter  $c_o$  is somewhat greater than  $c = 2.6$  for the first wave in Israel, and the intensity of hard measures,  $a_o$ , is much smaller than  $a$ . The significant drop of  $a$  can be possibly expected;  $1/\sqrt{a}$  is directly related to the duration of the wave.

We recall that the first wave in Israel matched well our  $u$ -curve, and this wave was managed efficiently. This was under strict lockdowns. The management of the first wave in the USA was not that steady. Opening schools in August-September is one of the key unknown factors, but not the only one of course. Also, a significant increase of the number of new daily cases in Europe at the end of vacation periods was expected; this really happened.

The starting number of the total cases for the second wave in the USA at 6/15 was 2.1M; the red dots were till 7/14, and the control black dots closely follow the  $u$ -curve till about 7/27. Upon subtracting 2.1M, one has:  $a_o = 0.06$ ,  $c_o = 2.65$ ,  $C_o = 3.4$ ,

$$u_{1,2}^o(t) = 3.4 t^{(c_o+1)/2} J_{\pm \frac{c_o-1}{2}}(\sqrt{a_o}t), \quad u_o(t) = u_1^o(t) + 0.6u_2^o(t).$$

Here we use our second Bessel-type solution  $u_o^2$ , so the connection of  $c_o$  with  $c = 2.2$  for the first wave (obtained without  $u^2$ ) is not that direct. We used  $u^2$  for Israel too, but its coefficient was small: 0.1.

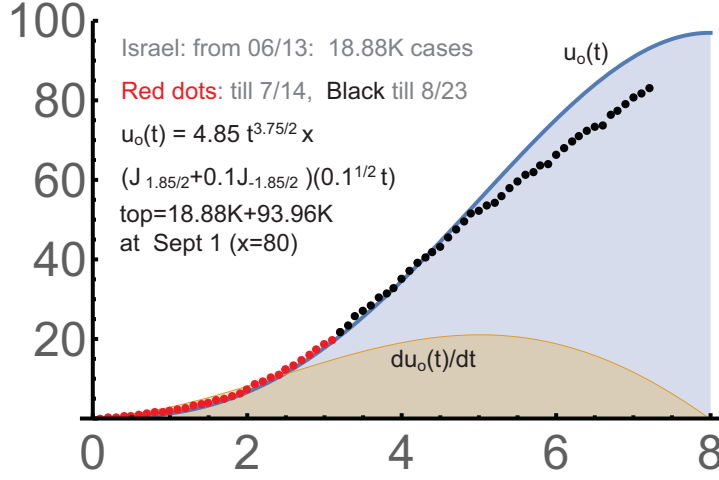


FIGURE 23. Second wave in Israel: 6/13-8/23.

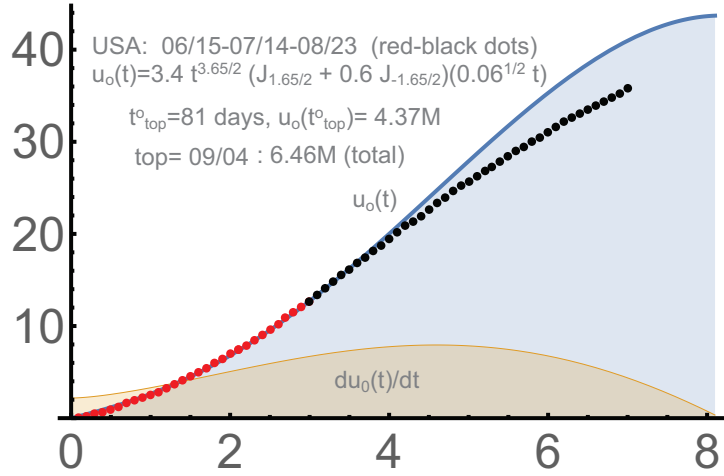


FIGURE 24. Second wave in the USA: 6/15-8/23.

Generally, finding  $a, c, C$  in the *early stages* and using them for some *preliminary* forecasting seems more reasonable *without*  $u^2$ , even if the latter gives a somewhat better match with the "red dots". The usage of  $u^2$  mainly addresses the presence of some bulges, i.e. some effects of "second order".

Generally, finding the optimal parameters which are stable enough, requires at least passing the "turning points". This is fully applicable to  $a$ , but the parameter  $c$ , the transmission coefficient in our theory, can be seen well in the early stages.

We note that the presence of wave 1 can generally make modeling wave 2 challenging mathematically. According to [Ch1], hypergeometric functions may be necessary. However, it appeared that simple subtracting "the pedestal" from the first wave made the Bessel functions sufficient to model the second wave in the USA: Figure 24.

The similarity of the curves of total cases in Israel and the USA considered above is interesting. This is for the second wave and the situations are very different in these countries. Nevertheless, the curves almost coincide upon some rescaling. The second interesting feature is that we see at the end of July a pattern in these curves similar to the switch from phase 1 to phase 2 we observed in many countries during the first wave. For instance, see Figure 15. This resulted in some passage to phase 2 in the USA, but not in Israel.

The situation is of course very fluid, the levels of new cases are high in both countries, and there is uncertainty with the beginning of the Fall there and everywhere. Then the developments were different in both countries. The USA basically reached phase 2 as of 09/13; many schools and business were closed. Israel's curve went up significantly and eventually this country enforced a total lockdown.

**13. Conclusion.** The main result of this paper is that the curves of the total numbers of detected infections of *Covid-19* can be described with high accuracy by our "two-phase solution". Let us provide one more confirmation. It appeared that Figure 24 extended to September 13 matches very well our formula for proper parameters. As for 9/20, the trend was toward some linear growth of the total number of cases, but the applicability of our two-phase solution to the second waves of this epidemic is of course an important argument in favor of the validity of our approach.

Let us provide some account of the projections for the USA we obtained during several stages:

- (1) in contrast to almost all Europe, the initial  $u$ -curve presented in Figure 1 with the saturation  $t_{top}$  at 5/5 did not work for the USA;
- (2) the switch to mode  $(AB)$  and the corresponding  $w$ -curve with the saturation at 5/30 in Figure 7 did not work too, in contrast to UK;
- (3) the projection "9/19" from Figure 20, based on the fact that  $\sim 22$  states reached phase 2 in June, did not materialized as well.

A very good match with our Bessel-type solution for the total number of detected cases in the USA in the middle of phase 1 of the first wave was the reason to expect (1) or (2), by analogy with many counties in Europe and some in Asia. The match was good for quite some time, ... before the hard measures were significantly relaxed. The projection in (3) was quite stable, but the next *dramatic* reduction of hard measures

in almost all 50 states made the saturation at 9/19 unlikely; the number of states in phase 2 quickly dropped from 22 to 8, and the USA entered the second wave. It was supposed to be similar to Figure 21 for Europe, but this did not happen.

With these 3 instances, the "pattern" is basically the same: *hard measures were relaxed upon the first signs of improvements, well before sufficiently small numbers of new daily cases were reached*. There are of course serious reasons for such a reduction, and this is applicable not only to the USA.

We mention that this kind of "early response" sometimes works well, for instance with *contrarian investing strategies*. However, professional investing is based on the earliest possible access to the news and predicting "mass behavior". Here we face something different.

Having the 2nd wave on top of the "unfinished" first is of course a negative development. Monitoring new infections, treating those infected, and general control of the situation become significantly less doable. Obviously, the likelihood of such a pattern exists in quite a few countries, Brazil and India included.

Clear second waves were present in the middle of July in 15+ countries and now (the middle of September) are quite common in Europe. It is likely that our differential equations and Bessel-type solutions describe them with the same kind of accuracy, as for the first waves. As it was predicted, they appeared right after the end of the first ones and their shape and the strength were quite comparable with those of the first waves.

Regardless of our theory, this confirms that "hard measures" were the main reason for the saturation of *Covid-19* in many countries. The second waves are quite common in epidemics, but they cannot be so soon if the process is "natural", i.e. not under intensive management.

Mathematical understanding the epidemic spread and forecasting the results of their management obviously deserve a systematic theory. In this paper, we mostly focus on the uniformity of the spread of *Covid-19* in many countries, namely, on the uniformity of the curves of total numbers of detected infections, which appeared very surprising. We think that our approach explains this.

There are not many different modes of epidemic management and the ways to "measure" the epidemic dynamics. Similar management, if it is the key factor, can be expected to result in similar features of the epidemic spread, including the curves of total cases, the saturation, the passage from phase one to phase two, and the second waves.

Every country has of course its own path during *Covid-19*. There can be *several* different patterns here (not just one), so a final theory will be ramified. The results of our theoretical and numerical analysis suggest that by now we have the following major ones:

- (a) The *West-European pattern*, with a successful path to the saturation of both phases and modeled very well by our "2-phase solution";
- (b) the *USA pattern*, similar to (a), but with as early reductions of hard measures as possible, which significantly delays the saturation;
- (c) "*Brazil-India*", with high  $c$ , replacing  $R_0$  in our theory, and with long stages of strong polynomial growth of the curves of total cases.

Let us update Figure 12 till 10/07/2020. The parameters there were determined *before* the turning point, so they were not that reliable. As of the beginning of November, India presumably reached this point. Interestingly, only  $c$  required some adjustment; it is now  $c = 5.75$  vs  $c = 5.2$  determined for the period till 8/23. *All other coefficients, including the exponent are unchanged.* The same (brown) power function  $0.0125(t+0.07)^{3.65}$  provided a good approximation till the turning point. The match with our Bessel-type solution was almost perfect, though of course much will depend on the further developments in India. Recall that  $y = \text{cases}/10K$  in Fig. 25. The red dots are those used in Figure 12 (till 8/23). The clear polynomiality of the curve of total cases in India and the match with our  $u$ -functions are of course important confirmations of our theory. We have:

$$u(t) = 0.55 t^{c/2+0.5} \left( J_{c/2-0.5}(\sqrt{at}) + 0.2 J_{0.5-c/2}(\sqrt{at}) \right), c = 5.75, a = 0.035.$$

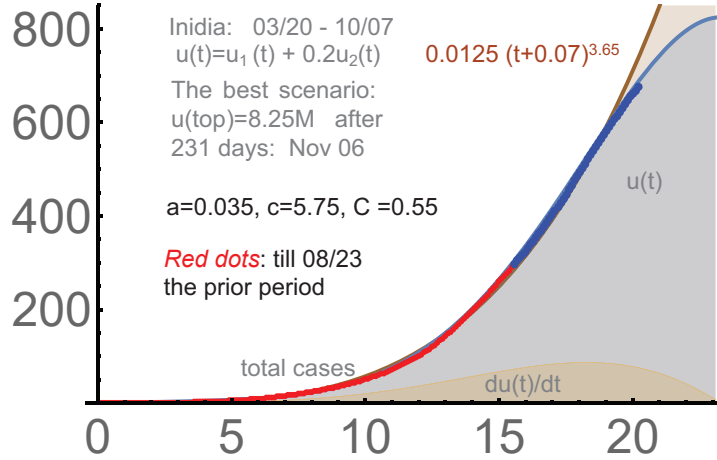


FIGURE 25. *India* : 3/20–10/7,  $c=5.75$ ,  $a=0.035$ ,  $C=0.55$ .

Automated modeling epidemics based on our "2-phase solution" followed by their automated forecasting is quite a challenge. This seems doable by analogy with the algorithms described in [Ch1] for trading stocks, which are working programs. For phase 2, our software can manage automatically (one-click) any groups of countries. This is not

an *AI-type* system so far, with self-learning and so on, but already quite efficient to monitor daily the *later* stages of *Covid-19*.

For the "end-users", our (or any) projections must be constantly renewed on the basis of the latest data. However it is very important to test the forecasts without any later adjustments and during sufficiently long periods; we do this systematically in this paper. The testing periods are the black and blue dots in our graphs.

It is of course important that our theory was created in the middle of the epidemic; this provides almost a unique chance to test it real-time. Real-time experiments are a must for forecasting and trading systems in stock markets. No models can be accepted there without such runs and carefully crafted tests excluding any usage of "future". This kind of discipline is not present in forecasting epidemics.

It is not unusual when the epidemic curves are approximated piecewise using frivolous choices of formulas and parameters. For *Covid-19*, the curves for the numbers of total cases can be presented as piecewise polynomial functions with fluctuating exponents, but this only confirms that their growth is no greater than polynomial.

Our  $u$ -curves used for phase 1 depend only on two major parameters, the initial transmission rate  $c$ , which can be seen in the early stages, and the intensity,  $a$ , of the measures employed. If  $u^2$  is used, then its coefficient is the third one, but this is mostly needed to address some "effects of second order".

Forecasting epidemics is of course a natural aim, but mathematical models are sometimes considered "acceptable" even if they are disconnected with real epidemic data. For instance, the usage of  $R_0$ , the *reproduction number*, is common in the literature in spite of the fact that the exponential growth of the number of cases can be observed only during very short periods, if any. The usage of the statistical tools and random processes is important, but only after the basic differential or difference equations are proved to be applicable.

To conclude, any forecasting required and requires mathematics. Any analysis or discussion of such complex events as epidemics must be based on strict definitions. For instance, comparing different countries and various phases is impossible without solid mathematical methods. This is fully applicable to understanding the efficiency of the measures employed, which can be a difficult task even if the corresponding mathematical tools are adequate.

Modeling the spread of *Covid-19* appeared closely related to the Bessel functions, which can be a challenge for researches in the field of mathematical epidemiology. The theory of these functions, introduced by Daniel Bernoulli and generalized by Bessel, was renewed recently. We actually use some recent developments, but the final formulas require only very basic "one-line" definitions, simple to use practically.



Their quasi-periodicity is a deep classical result, which provides a brand new approach to the saturation of epidemics under active management. In contrast to the saturation due to the *herd immunity* or biological factors, this kind of saturation, the main one for *Covid-19*, is of unstable nature and does require thorough mathematical theory. This paper is the first step in this direction.

**Acknowledgements.** I thank very much David Kazhdan for valuable comments and suggestions; a good portion of this paper presents my attempts to answer his questions. I also thank Eric Opdam and Alexei Borodin for their kind interest, and the referee for useful suggestions. I'd like to thank ETH-ITS for outstanding hospitality; my special thanks are to Giovanni Felder, Rahul Pandharipande.

**14. Appendix: auto-forecasting.** We will discuss the usage of the programs designed for forecasting late stages of the waves of *Covid-19* in any countries or groups of countries. They are available as the supplement to the published version of this work; see also [Ch2]. The second wave of *Covid-19* in the USA is considered in detail; our 2-phase solution appeared applicable.

**Forecasting late stages.** The programs are designed to be used only at later stages of (the waves of) *Covid-19* in any countries, groups of countries, and regions. We provide a "universal program" (any countries) in FOREU.zip, and its version in FORUS.zip designed for the USA via auto-forecasting the spread in all 50 states and calculating the *superposition* of the corresponding projections. These programs are based on the type *B* formulas for  $u_B(t)$ , which were used in our *2-phase solution*. They describe *only* later stages: phase two in our terminology.

The "universal program" gave quite stable results for Western Europe, but only till the middle of August. Then the second wave began there, presumably due to the end of vacations and the beginning of the school year. The USA program (all states separately) provided stable projections for the saturation till the middle of June, the beginning of the second wave in the USA. Then a significant reduction of the hard measures began. It appeared applicable again in the beginning of September in the USA, with a path to the saturation of the second wave.

The fact that many schools and businesses were closed in the USA, in contrast to Europe, contributed to this. However the trend changed in the middle of September: the number of new daily cases became essentially constant, which corresponds to a linear growth of the number of total cases. In Europe, a strong growth of the total number of (detected) cases began in the end of August, so the program became essentially a linear approximation in September.

**Two outputs.** The "universal program" starting with about 9/20 gave the linear approximation for the total number of infections. We provide the output of 9/23 in Figure 26. The projections are for 3 months from the date if the saturation cannot be found during this period.

The second program, based on the consideration of all 50 states, is presumably more reliable. The first run we provide is as of 9/12. The projection was 5.8M in the first 2 weeks of December on top of the initial 2.1M at 06/16. Actually, only about 17 States were in phase 2, so this was not really reliable. This number dropped to about 11 on 9/22. The program still found the saturation for the 9-day average of the corresponding curves but it was 12/28. The trend was toward the linear growth of the total number of cases.

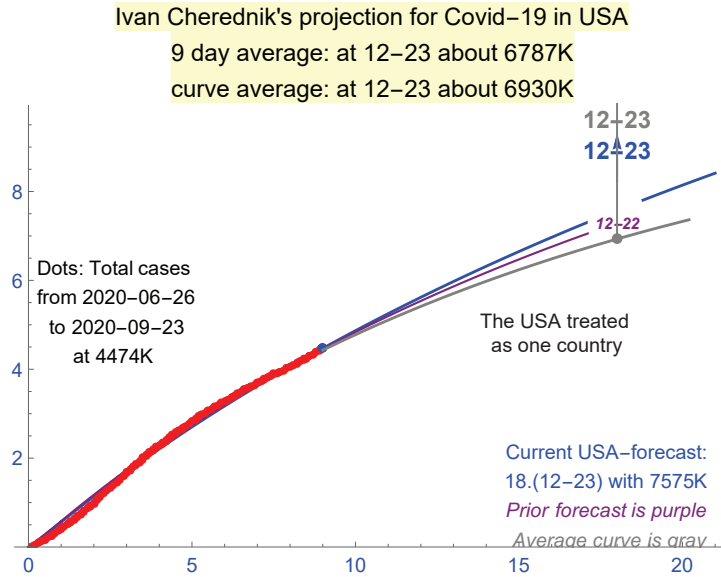


FIGURE 26. Universal forecast: not via 50 States.

Any reopening of schools and businesses in the USA can and will influence these projections, as occurred in Europe. This already happened in the middle of June, when the USA approached the second phase of the 1st wave, after the hard measures were significantly reduced. Much depends on the virus evolution too. Let us provide two outputs of the program for the USA: Figures 27, 28.

**Two phase-solution.** This solution worked well at least till the middle of September for the second wave in the USA. The accuracy is comparable with what we obtained and discussed in this paper for the first waves in Japan, Israel, Italy, Germany, UK and the Netherlands. Upon subtracting 2.1M, the parameters we obtained for the early-middle stage

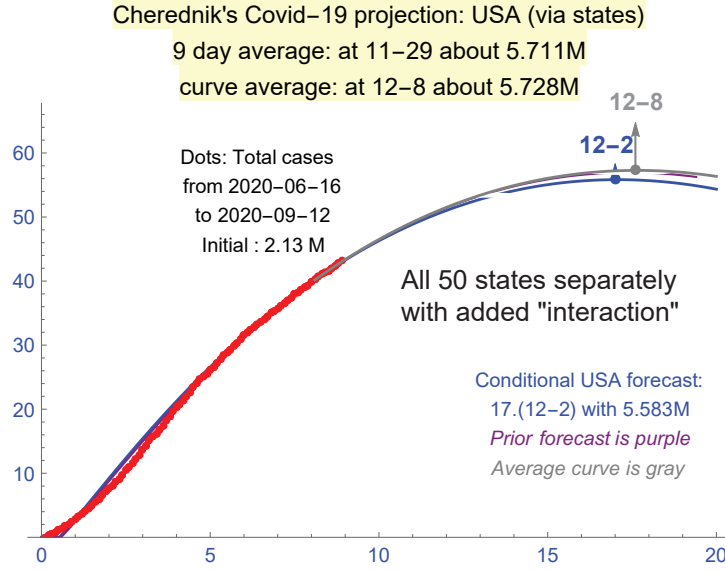


FIGURE 27. All 50 states separately (9/12).

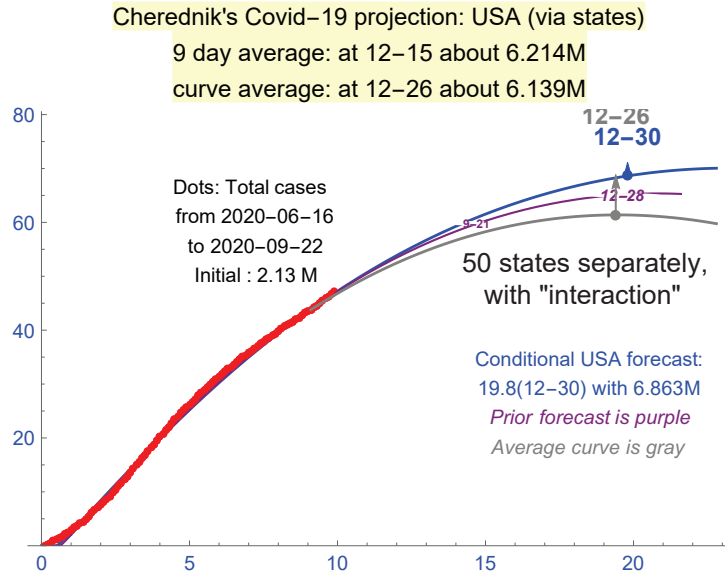


FIGURE 28. All 50 states separately (9/22).

of the 2nd wave in the USA were:  $a_o = 0.06$ ,  $c_o = 2.65$ ,

$$u_{1,2}^o(t) = 3.4 t^{(c_o+1)/2} J_{\pm \frac{c_o-1}{2}}(\sqrt{a_o}t), \quad u_o(t) = u_1^o(t) + 0.6u_2^o(t).$$

The second phase matched well the following function:

$$u_B(t) = 4.1 t^{c/2} \cos(d \log(\text{Max}(1, t))), c=2.65, d=0.435.$$

The projected saturation for  $u_B$  was given by the formula  $t_{\text{end}} = \exp(\frac{1}{d} \tan^{-1}(\frac{c}{2d}))$ . Numerically,  $t_{\text{end}} = 17.8463$ , which is 178 days from 06/16: December 11, 2020. See Figure 29. This date basically matches the auto-projection based on considering all 50 states separately in Figures 27, 28. However, the latter are actually the last ones before the growth of the number of total cases became linear in the USA.

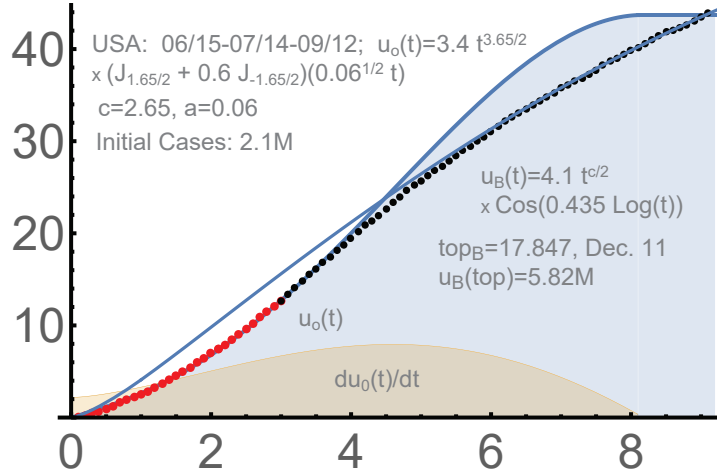


FIGURE 29. 2-phase solution for the 2nd wave in the USA.

**Practical matters.** The main programs in *FOREU.zip* are "forwor.txt" and "forworstat.txt". In Mathematica, run "forwor.txt"; it is set for the United States. Upon making  $grp = 0$  in "worldfile.txt", it will work for Europe. Some countries were excluded in Europe, mostly due to problems with data. To change this you need to open "forwor.txt" and "forworstat.txt" and find the corresponding places. Mathematica programs are readable.

Generally, the program is "one-click": run the exe-file, after you adjust the path to "math.exe" in your computer in the file "math-path.txt", and set the countries/regions in "worldfile.txt" following the "README" file.

This is similar for the program for 50 states in the USA. There is no file "worldfile.txt", and currently all states are included. The initial date is set to 06/16/2020. This can be adjusted directly in "forusa.txt" and "forustat.txt": change "datein" (all instances).

The initial date is automatically set to 3 months before "today" in the universal program (for any countries), but not in this one. Here it is the beginning of the wave.

Mathematica 11 is necessary to use these programs. For the universal program, `raw.githubusercontent.com/owid/covid-19-data/` is used: the online access to this site is needed. The names of the countries and regions in "worworld.txt" must be as at this site. The site `raw.githubusercontent.com/nytimes/covid-19-data/` is used for the program managing the 50 states in the USA.

The *saturation* in these programs is technical; it is supposed to move over time. If the program detects no saturation, then the projections will be provided for a 4 month period; in this case, the program mostly works as a linear extrapolation.

The programs are not for any commercial use; the name of their creator, Ivan Cherednik, and a link to the Journal or [Ch2] must be always provided. This is a research tool only. The source file in Mathematica is readable, so you can understand what the programs really do. Please see the README-files.

## References.

- [CJLP] R. Carrasco-Hernandez, and R. Jácome, and Y. López Vidal, and S. Ponce de León, *Are RNA viruses candidate agents for the next global pandemic? A review*, ILAR Journal, 58:3 (2017), 343–358. [8](#)
- [CLL] M. Castro, and M. López-Garcia, and G. Lythe, and et al, *First passage events in biological systems with non-exponential inter-event times*, Sci Rep 8, 15054 (2018), doi.org/10.1038/s41598-018-32961-7. [5](#), [24](#)
- [Ch1] I. Cherednik, *Artificial intelligence approach to momentum risk-taking*, Preprint: arxiv 1911.08448v4 (q-fin), 2019. [5](#), [9](#), [10](#), [11](#), [17](#), [18](#), [23](#), [45](#), [47](#)
- [Ch2] — , *A surprising formula for the spread of Covid-19 under aggressive management*, Preprint: medRxiv, doi: 10.1101/2020.04.29.2008448 , 2020. [5](#), [49](#), [53](#)
- [Che] P. Cheridito, *Mixed fractional Brownian motion*, Bernoulli 7 (2001), 913–934. [18](#)
- [Co] S. Cobey, *Modeling infectious disease dynamics*, Science, 24 Apr 2020; DOI: 10.1126/science.abb5659. [8](#)
- [He] H. Hethcote, *The mathematics of infectious diseases*, SIAM Review, 42:4. (2000), 599–653. [6](#)
- [HL] H. Hethcote, and S. Levin, *Periodicity in Epidemiological Models*, In: Applied Mathematical Ecology. Biomathematics, 18, 193–211, Springer, Berlin, Heidelberg, S. Levin, T. Hallam, L. Gross (eds), 1989. [7](#), [24](#)
- [Kat] M. Katori, *Bessel process, Schramm-Loewner evolution, and Dyson model*, Preprint: arxiv 1103.4728v1 (2011). [18](#)
- [MH] S. Meyer, and L. Held, *Power-Law models for infectious disease spread*, The Annals of Applied Statistics 8:3 (2014), 1612–1639. [23](#)
- [St] Ph. Strong, *Epidemic psychology: a model*, Sociology of Health & Illness 12:3 (1990), 249–259. [6](#)
- [Wa] G.N. Watson, *A Treatise on the Theory of Bessel Functions*, 2nd Edition, Cambridge University Press, Cambridge, 1944. [16](#)

(I. Cherednik) DEPARTMENT OF MATHEMATICS, UNC CHAPEL HILL, NORTH  
CAROLINA 27599, USA, CHERED@EMAIL.UNC.EDU